

Randomized Riemannian Preconditioning for Quadratically Constrained Problems

Boris Shustin

Haim Avron

Tel Aviv University

BORISSHY@MAIL.TAU.AC.IL

HAIMAV@TAUEX.TAU.AC.IL

Abstract

Optimization problem with quadratic equality constraints are prevalent in machine learning. Indeed, two important examples are Canonical Correlation Analysis (CCA) and Linear Discriminant Analysis (LDA). Unfortunately, methods for solving such problems typically involve computing matrix inverses and decomposition. For the aforementioned problems, these matrices are actually Gram matrices of input data matrices, and as such the computations are too expensive for large scale datasets. In this paper, we propose a sketching based approach for solving CCA and LDA that reduces the cost dependence on the input size. The proposed algorithms feature randomized preconditioning combined with Riemannian optimization.

Keywords: Riemannian Optimization, Sketching, Numerical Linear Algebra, CCA, LDA

1. Introduction

Large scale machine learning often requires some form of dimensionality reduction in order to accelerate the solution of computations that are otherwise too costly, and matrix sketching has recently emerged as a powerful technique for such dimensionality reduction. There are generally, two approaches for leveraging sketching: sketch-and-solve and sketch preconditioning (see Section 2.3). Sketch-and-solve is more prevalent in the literature, but is unable to deliver high accuracy approximations. In contrast, sketch preconditioning (also called randomized preconditioning), when viable, is able to deliver highly accurate results, close to the quality of the exact solution¹. Unfortunately, developing algorithms based on randomized preconditioning is more challenging due to the need for an underlying preconditioned iterative method, and so far randomized preconditioning has essentially been limited to regression problems.

In this paper, we consider using randomized preconditioning in the context of optimization problems with quadratic equality constraints. That is, we consider problems of the form

$$\min f(\mathbf{x}_1, \dots, \mathbf{x}_k) \text{ s.t. } \mathbf{x}_i^T \mathbf{B}_i \mathbf{x}_i = 1 \ (i = 1, \dots, k) \quad (1)$$

where $\mathbf{B}_1, \dots, \mathbf{B}_k$ are fixed symmetric positive definite matrices (SPD), given in an implicit form as the Gram matrix of input datasets. Such problems naturally arise in quite a few applications:

1. Finding the eigenvector corresponding to the smallest eigenvalue of a symmetric positive definite matrix \mathbf{A} corresponds to solving $\max \mathbf{x}^T \mathbf{x}$ s.t. $\mathbf{x}^T \mathbf{A} \mathbf{x} = 1$. One possible application

1. That said, there are other metrics in which the sketch-and-solve is potentially superior to the sketch preconditioning approach; a complete comparison between the two approaches is outside the scope of this paper.

is low rank approximation of the inverse of a covariance matrix, i.e. the precision matrix, in which case \mathbf{A} is the Gram matrix of the input data.

2. Suppose \mathbf{A} and \mathbf{B} are two symmetric positive definite matrices. The eigenvector corresponding to the largest generalized eigenvalue is the solution of $\max \mathbf{x}^T \mathbf{A} \mathbf{x}$ s.t. $\mathbf{x}^T \mathbf{B} \mathbf{x} = 1$. One example application is Linear Discriminant Analysis (LDA), in which \mathbf{B} is the Gram matrix of a shifted version of the input data.
3. Let $\mathbf{X} \in \mathbb{R}^{n \times d_x}$ and $\mathbf{Y} \in \mathbb{R}^{n \times d_y}$ be two data matrices, and let $\lambda_x, \lambda_y \geq 0$ be two regularization parameters. In Canonical Correlations Analysis (CCA) we seek to find a $\mathbf{u} \in \mathbb{R}^{d_x}$ and a $\mathbf{v} \in \mathbb{R}^{d_y}$ that maximize $\mathbf{u}^T \mathbf{X}^T \mathbf{Y} \mathbf{v}$ subject to $\mathbf{u}^T (\mathbf{X}^T \mathbf{X} + \lambda_x \mathbf{I}_{d_x}) \mathbf{u} = 1$ and $\mathbf{v}^T (\mathbf{Y}^T \mathbf{Y} + \lambda_y \mathbf{I}_{d_y}) \mathbf{v} = 1$.

Sketch-and-solve approaches have been applied to the aforementioned problems, or close variants of them. For example, [Avron et al. \(2014a\)](#) developed a sketch-and-solve approach for CCA. In this paper, we aim to develop randomized preconditioners for optimization problems with quadratic equality constraints. For concreteness, we focus only on the CCA and LDA problem, although we expect our technique to be more generally applicable. Let us now summarize our contributions:

- The constraints in Eq. (1) form a smooth manifold, so Riemannian optimization ([Smith, 1994](#)), is naturally suited for such problems. Metric selection (for the manifold) can be used to incorporate preconditioning. To facilitate this, we develop the necessary geometrical components required to optimize on manifolds corresponding to the quadratic equality constraints using non-standard metric selection. These developments are reported in Section 3.
- We use the tools developed in Section 3 to propose preconditioned iterative methods for CCA and LDA. We theoretically analyze the effect of the preconditioner on the asymptotic convergence rate, and identify the optimal preconditioner. These results are reported in Section 5.
- We show how sketching can be used to form effective preconditioners in context of the generic algorithms developed in Section 5. We then develop end-to-end sketching based algorithms for CCA and LDA. We report numerical experiments supporting the viability of randomized preconditioning for CCA and LDA. These results are reported in Section 6 and in Appendix D.

Due to space constraint, discussion of related work is deferred to the appendix.

2. Preliminaries

2.1. Notation and Basic Definitions

We denote scalars using lower case Greek letters or using x, y, \dots . Vectors are denoted by $\mathbf{x}, \mathbf{y}, \dots$ and matrices by $\mathbf{A}, \mathbf{B}, \dots$ or upper case Greek letters. Tangent vectors (of a manifold) are denoted using lower case Greek letters with a subscript for the point of the manifold for which they correspond (e.g. $\eta_{\mathbf{x}}$). The $s \times s$ identity matrix is denoted \mathbf{I}_s . We use the convention that vectors are column-vectors. $\text{nnz}(\mathbf{A})$ denotes the number of non-zeros in \mathbf{A} . We denote by $(\cdot, \cdot)_{\mathbf{M}}$ the inner-product with respect to a matrix \mathbf{M} : $(\mathbf{u}, \mathbf{v})_{\mathbf{M}} := \mathbf{u}^T \mathbf{M} \mathbf{v}$.

Let \mathbf{A} be a symmetric $d \times d$ matrix. We use $\lambda_1(\mathbf{A}) \geq \lambda_2(\mathbf{A}) \geq \dots \geq \lambda_d(\mathbf{A})$ to denote the eigenvalues of \mathbf{A} , and use $\kappa(\mathbf{A})$ to denote the *condition number* of \mathbf{A} , which is the ratio between

the largest and smallest eigenvalues in absolute value. Let $\mathbf{B} \in \mathbb{R}^{d \times d}$ be another symmetric positive semidefinite matrix, and assume that $\ker(\mathbf{B}) \subseteq \ker(\mathbf{A})$. If for $\lambda \in \mathbb{R}$ and $\mathbf{v} \notin \ker(\mathbf{B})$ it holds that $\mathbf{A}\mathbf{v} = \lambda\mathbf{B}\mathbf{v}$ then λ is a *generalized eigenvalue* and \mathbf{v} is a *generalized eigenvector* of the *matrix pencil* (\mathbf{A}, \mathbf{B}) . We use the notation $\lambda_1(\mathbf{A}, \mathbf{B}) \geq \lambda_2(\mathbf{A}, \mathbf{B}) \geq \dots \geq \lambda_{\text{rank}(\mathbf{B})}(\mathbf{A}, \mathbf{B})$ to denote the generalized eigenvalues of (\mathbf{A}, \mathbf{B}) . The (generalized) condition number $\kappa(\mathbf{A}, \mathbf{B})$ of the pencil (\mathbf{A}, \mathbf{B}) is the ratio the largest and smallest generalized eigenvalues in absolute value. If \mathbf{B} is also non-singular, that is \mathbf{B} is a symmetric positive definite (SPD) matrix, then it holds that $\kappa(\mathbf{A}, \mathbf{B}) = \kappa(\mathbf{B}^{-1/2}\mathbf{A}\mathbf{B}^{-1/2}) = \kappa(\mathbf{B}^{-1}\mathbf{A})$.

For a SPD matrix $\mathbf{B} \in \mathbb{R}^{d \times d}$ we denote by $\mathbb{S}^{\mathbf{B}}$ the $d - 1$ dimensional ellipsoid defined by

$$\mathbb{S}^{\mathbf{B}} := \left\{ \mathbf{x} \in \mathbb{R}^d : \mathbf{x}^T \mathbf{B} \mathbf{x} = 1 \right\}.$$

$\mathbb{S}^{\mathbf{B}}$ is a $d - 1$ dimensional submanifold of \mathbb{R}^d . Given a function or vector field defined on $\mathbb{S}^{\mathbf{B}}$, we use a bar decorator to denote a smooth extension of that object to the entire \mathbb{R}^d , either by committing to a specific extension, or making sure that the following statements hold for *any* smooth extension. For example, given a smooth objective $f : \mathbb{S}^{\mathbf{B}} \rightarrow \mathbb{R}$, we use $\bar{f} : \mathbb{R}^d \rightarrow \mathbb{R}$ to denote a smooth real-valued function defined on \mathbb{R}^d whose restriction to $\mathbb{S}^{\mathbf{B}}$ is f .

2.2. Riemannian Optimization

Riemannian optimization provides a principled approach for adapting unconstrained optimization algorithms, to solve constrained optimization problems in which the constraints form a smooth manifold (e.g., nonlinear differentiable equality constraints). A detailed introduction can be found in [Absil et al. \(2009\)](#). Here we recall some basic definitions, and establish corresponding notations.

A *Riemannian manifold* (\mathcal{M}, g) is a real differentiable manifold \mathcal{M} with a smoothly varying inner product $g_{\mathbf{x}}$ on *tangent spaces* $T_{\mathbf{x}}\mathcal{M}$ (where $\mathbf{x} \in \mathcal{M}$). The inner product is referred to as the *Riemannian metric*. Crucially, the inner product can depend on $\mathbf{x} \in \mathcal{M}$. We say that a Riemannian manifold (\mathcal{M}, g) is a *Riemannian submanifold* of another Riemannian manifold $(\bar{\mathcal{M}}, \bar{g})$, if \mathcal{M} is a submanifold of $\bar{\mathcal{M}}$ and it inherits the metric in a natural way: $g_{\mathbf{x}}(\eta_{\mathbf{x}}, \xi_{\mathbf{x}}) = \bar{g}_{\mathbf{x}}(\eta_{\mathbf{x}}, \xi_{\mathbf{x}})$ for $\eta_{\mathbf{x}}, \xi_{\mathbf{x}} \in T_{\mathbf{x}}\mathcal{M}$ where in the right-side $\eta_{\mathbf{x}}$ and $\xi_{\mathbf{x}}$ are viewed as elements in $T_{\mathbf{x}}\bar{\mathcal{M}}$ (this is possible since \mathcal{M} is a submanifold of $\bar{\mathcal{M}}$).

The notion of *retraction* (Section 4.1 in [Absil et al. \(2009\)](#)) allows us to take step at point $\mathbf{x} \in \mathcal{M}$ in a direction $\xi_{\mathbf{x}} \in T_{\mathbf{x}}\mathcal{M}$: a map $R_{\mathbf{x}} : T_{\mathbf{x}}\mathcal{M} \rightarrow \mathcal{M}$ is a retraction if it upholds a local rigidity condition. The notion of *vector transport* (Section 8.1 in [Absil et al. \(2009\)](#)) is useful for manipulating tangent vectors from two different tangent spaces. In particular, $\mathcal{T}_{\eta_{\mathbf{x}}}(\xi_{\mathbf{x}})$ for $\eta_{\mathbf{x}}, \xi_{\mathbf{x}} \in T_{\mathbf{x}}\mathcal{M}$ transports $\xi_{\mathbf{x}}$ from $T_{\mathbf{x}}\mathcal{M}$ to $T_{R_{\mathbf{x}}(\eta_{\mathbf{x}})}\mathcal{M}$.

The notions of Riemannian gradient and Riemannian Hessian (Sections 3.6 and 5.5 in [Absil et al. \(2009\)](#)) generalize the corresponding concepts from the Euclidean setting. For a function $f : \mathcal{M} \rightarrow \mathbb{R}$, we denote the Riemannian gradient and Riemannian Hessian at $\mathbf{x} \in \mathcal{M}$ by $\mathbf{grad} f(\mathbf{x}) \in T_{\mathbf{x}}\mathcal{M}$ and $\mathbf{Hess} f(\mathbf{x}) : T_{\mathbf{x}}\mathcal{M} \rightarrow T_{\mathbf{x}}\mathcal{M}$ respectively. Roughly speaking, the *Levi-Civita* or *Riemannian connection* ∇ of (\mathcal{M}, g) allows us to generalize the notion of directional derivative of vector fields. We use $\mathfrak{X}(\mathcal{M})$ to denote the set of vector fields on \mathcal{M} .

With these components, various optimization algorithms naturally generalize. For example, one possible Riemannian gradient method is given by the formula

$$\mathbf{x}_{k+1} = R_{\mathbf{x}_k}(\tau_k \mathbf{grad} f(\mathbf{x}_k)) \quad (2)$$

where τ_k is the step size (possibly chosen by the *Armijo's backtracking procedure*). In our experiments, we use Riemannian Conjugate Gradient (Absil et al., 2009, Algorithm 13) and Riemannian Trust Region (Absil et al., 2009, Algorithm 10). MANOPT is a MATLAB library that implements these, and other, Riemannian optimization algorithms (Boumal et al., 2014).

2.3. Sketching and Randomized Preconditioning

Matrix sketching is a dimensionality reduction technique for accelerating and improving matrix computations which naturally arise in statistical learning such as linear regression, low rank approximation, and principal component analysis (see surveys by Woodruff et al. (2014), Yang et al. (2016)). Roughly speaking, the core idea is to embed a high dimensional space in a lower dimension space, while preserving some properties of the high dimensional space (Drineas et al., 2011).

There are two dominant approaches for utilizing matrix sketching. The first, often referred to as “sketch-and-solve”, attempts to find a good approximate solution by sketching the input data such that with high probability the exact solution of the sketched problem is a good approximate solution to the original problem. In the context of this paper, worth mentioning is a recent paper that suggested a sketch-and-solve based algorithm for CCA (Avron et al., 2014a). The second approach is “sketch preconditioning” (also called “randomized preconditioning”), where the main idea is to use a sketched matrix of the input data to form a preconditioner, for example by some factorization, then the preconditioner is used in an iterative method. For example, it is possible to accelerate the solution of least squares problems of the form $\min_{\mathbf{x}} \|\mathbf{Ax} - \mathbf{b}\|_2$ by sketching the matrix \mathbf{A} to form \mathbf{SA} , and use \mathbf{SA} to form a preconditioner for an iterative Krylov method (e.g., LSQR) (Avron et al., 2010; Meng et al., 2014; Clarkson and Woodruff, 2017; Gonen et al., 2016).

Although there are quite a few works that employ the sketch preconditioning approach, the use of the sketch-and-solve approach is more prevalent in the literature. Possibly, since the sketch preconditioning approach requires an iterative method that can be preconditioned, and such a method is not always known for the various problems addressed by sketching. Indeed, most of the previous work on sketch preconditioning focused on regression and solving linear systems; these are cases where the use of preconditioning is straightforward. In this paper, we propose a randomized preconditioning strategy for problems involving quadratic equality constraints, such as CCA and LDA.

2.4. Preconditioning and Riemannian Preconditioning

In the context of solving a linear equation $\mathbf{Ax} = \mathbf{b}$, preconditioning is usually viewed as a manipulation of the linear system. For example, it is well known that when \mathbf{A} is SPD, the number of iterations until convergence of classical iterative methods (CG, MINRES, Richardson,...) depend on the condition number $\kappa(\mathbf{A})$ of the matrix. Thus, by multiplying the equation by \mathbf{M}^{-1} , we get a new system $\mathbf{M}^{-1}\mathbf{Ax} = \mathbf{M}^{-1}\mathbf{b}$ which has a different condition number $\kappa(\mathbf{M}^{-1}\mathbf{A})$. Thus, if that condition number is small (i.e. $\mathbf{M} \approx \mathbf{A}$), while \mathbf{M} is easy to factorize, then we can potentially achieve a computational advantage.

It is hard to leverage the aforementioned view of preconditioning if we want to go beyond solving linear equations, since it is not always clear how to manipulate the problem while changing the relevant condition number. Luckily, classical iterative methods are often an instance of Riemannian optimization, and preconditioning of classical iterative methods can be interpreted as a Riemannian

metric selection. As such, preconditioning of classical iterative methods is an instance of so-called Riemannian preconditioning (Mishra and Sepulchre, 2016).

To illustrate this, let's consider a concrete example. The solution of $\mathbf{Ax} = \mathbf{b}$ when \mathbf{A} is SPD is equivalent to the solution of $\min_{\mathbf{x} \in \mathbb{R}^d} \mathbf{b}^T \mathbf{x} - \frac{1}{2} \mathbf{x}^T \mathbf{Ax}$. The use of gradient descent to solve this problem leads to the iteration $\mathbf{x}_{k+1} = \mathbf{x}_k + \tau_k (\mathbf{b} - \mathbf{Ax}_k)$, which is well known as the *Richardson Iteration*. Now, if instead of using the dot product as the inner product on \mathbb{R}^d , we use the inner product $(\cdot, \cdot)_{\mathbf{M}}$ (which we view as a Riemannian metric on the manifold \mathbb{R}^d), the Riemannian gradient descent iteration becomes $\mathbf{x}_{k+1} = \mathbf{x}_k + \tau_k \mathbf{M}^{-1} (\mathbf{b} - \mathbf{Ax}_k)$. This new iteration is known as *Preconditioned Richardson Iteration*, and is classically derived as Richardson Iteration on $\mathbf{M}^{-1} \mathbf{Ax} = \mathbf{M}^{-1} \mathbf{b}$.

More generally, Riemannian preconditioning refers to the paradigm of preconditioning Riemannian optimization algorithms by judiciously selecting the metric endowed on the constraint manifold (Mishra and Sepulchre, 2016). Indeed, Mishra and Sepulchre (2016) show cases where one metric selection results in very slow convergence, while others lead to faster convergence. In this paper, we consider the manifold $\mathbb{S}^{\mathbf{B}}$, and precondition it using the inner product $(\cdot, \cdot)_{\mathbf{M}}$. For the problems we consider, the best convergence bounds are achieved when $\mathbf{M} = \mathbf{B}$, but that results in expensive algorithms due to the need to factorize \mathbf{B} . Thus, as is done when preconditioning linear solvers, there is a need to balance between goodness-of-approximation $\mathbf{M} \approx \mathbf{B}$, and cost of factorization of \mathbf{M} .

3. Geometry of the Ellipsoid

Our goal is to solve problems of the form $\min_{\mathbf{x} \in \mathbb{S}^{\mathbf{B}}} f(\mathbf{x})$ using Riemannian optimization. In this section we describe the necessary components required for Riemannian optimization on $\mathbb{S}^{\mathbf{B}}$, where we treat $\mathbb{S}^{\mathbf{B}}$ as an embedded submanifold of \mathbb{R}^d . In the following, we refer to \mathbb{R}^d as the *ambient space*. It is important to stress that all our formulas are given in ambient space coordinates, and not in some in some local coordinates of the manifold $\mathbb{S}^{\mathbf{B}}$.

3.1. Metric Independent Notions

The following lemma gives formulas (in ambient coordinates) for the metric independent notions: tangent spaces, retraction and vector transport. The proof of Lemma 1, and all other proofs, are deferred to Appendix E.

Lemma 1 *The tangent space at $\mathbf{x} \in \mathbb{S}^{\mathbf{B}}$, $T_{\mathbf{x}} \mathbb{S}^{\mathbf{B}}$, viewed as a subspace of $T_{\mathbf{x}} \mathbb{R}^d \simeq \mathbb{R}^d$, is*

$$T_{\mathbf{x}} \mathbb{S}^{\mathbf{B}} = \left\{ \mathbf{z} \in \mathbb{R}^d : \mathbf{z}^T \mathbf{B} \mathbf{x} = 0 \right\}. \quad (3)$$

The following defines a retraction on $\mathbb{S}^{\mathbf{B}}$ ($\mathbf{x} \in \mathbb{S}^{\mathbf{B}}$, $\xi_{\mathbf{x}} \in T_{\mathbf{x}} \mathbb{S}^{\mathbf{B}}$):

$$R_{\mathbf{x}}(\xi_{\mathbf{x}}) := \frac{\mathbf{x} + \xi_{\mathbf{x}}}{\|\mathbf{x} + \xi_{\mathbf{x}}\|_{\mathbf{B}}} \quad (4)$$

Finally, the following defines a vector transport on $\mathbb{S}^{\mathbf{B}}$ ($\mathbf{x} \in \mathbb{S}^{\mathbf{B}}$, $\eta_{\mathbf{x}}, \xi_{\mathbf{x}} \in T_{\mathbf{x}} \mathbb{S}^{\mathbf{B}}$):

$$\mathcal{T}_{\eta_{\mathbf{x}}}(\xi_{\mathbf{x}}) := \frac{1}{\|\mathbf{x} + \eta_{\mathbf{x}}\|_{\mathbf{B}}} \left[\mathbf{I} - \frac{(\mathbf{x} + \eta_{\mathbf{x}})(\mathbf{x} + \eta_{\mathbf{x}})^T \mathbf{B}}{\|\mathbf{x} + \eta_{\mathbf{x}}\|_{\mathbf{B}}^2} \right] \xi_{\mathbf{x}}. \quad (5)$$

3.2. Metric Related Notions

A crucial component for Riemannian optimization is the imposition of a Riemannian metric on the constraint manifold. The metric allows us to measure lengths of tangent vectors, and thus facilitate the definition of Riemannian gradient and related notions. The metric selection can have a substantial effect on the convergence properties of the optimization, and on the cost of each iteration, as we shall see in Sections 4 and 5. Thus, our preconditioning strategy relies on selecting an appropriate metric, hopefully balancing between fast convergence and cheap iterations.

Specifically, we define a Riemannian metric on the ambient space \mathbb{R}^d , and this uniquely defines a metric on $\mathbb{S}^{\mathbf{B}}$ that makes it a Riemannian submanifold. Similar to preconditioned methods in Euclidean space, the metric we define on \mathbb{R}^d is $\bar{g}_{\mathbf{x}}(\bar{\xi}_{\mathbf{x}}, \bar{\eta}_{\mathbf{x}}) := (\bar{\xi}_{\mathbf{x}}, \bar{\eta}_{\mathbf{x}})_{\mathbf{M}} = \bar{\xi}_{\mathbf{x}}^{\mathbf{T}} \mathbf{M} \bar{\eta}_{\mathbf{x}}$ where \mathbf{M} is some constant SPD matrix (which later takes the role of the preconditioner). In particular, for any $\mathbf{x} \in \mathbb{S}^{\mathbf{B}}$, $\xi_{\mathbf{x}}, \eta_{\mathbf{x}} \in T_{\mathbf{x}}\mathbb{S}^{\mathbf{B}}$, given in the coordinates of the ambient space, the metric on $\mathbb{S}^{\mathbf{B}}$ is given by $g_{\mathbf{x}}(\xi_{\mathbf{x}}, \eta_{\mathbf{x}}) = \xi_{\mathbf{x}}^{\mathbf{T}} \mathbf{M} \eta_{\mathbf{x}}$.

Remark 2 *The ellipsoid $\mathbb{S}^{\mathbf{B}}$ is a special case of the generalized Stiefel manifold. Classically, the metric employed for the generalized Stiefel manifold corresponds to $\mathbf{M} = \mathbf{B}$ (Edelman et al., 1998). However, as we shall see, various operations require products with \mathbf{M}^{-1} , and in our intended applications this results in algorithms that are too expensive.*

Riemannian Gradient. We find the gradient using Eq. (3.37) from (Absil et al., 2009). Let $f : \mathbb{S}^{\mathbf{B}} \rightarrow \mathbb{R}$ be smooth function, and let \bar{f} be a smooth extension (typically, f is given in ambient coordinates, thereby making the extension \bar{f} natural). The Riemannian gradient can then be found by computing the Riemannian gradient in \mathbb{R}^d of \bar{f} , and orthogonally projecting it with respect to the Riemannian metric to the tangent space of $\mathbb{S}^{\mathbf{B}}$. In short, $\text{grad} f(\mathbf{x}) = \mathbf{P}_{\mathbf{x}} \text{grad} \bar{f}(\mathbf{x})$ where $\mathbf{P}_{\mathbf{x}}$ is the orthogonal projection on $T_{\mathbf{x}}\mathbb{S}^{\mathbf{B}}$ with respect to $(\cdot, \cdot)_{\mathbf{M}}$. The following lemma gives a formula for $\mathbf{P}_{\mathbf{x}}$:

Lemma 3 *The orthogonal projection with respect to $(\cdot, \cdot)_{\mathbf{M}}$ on $T_{\mathbf{x}}\mathbb{S}^{\mathbf{B}}$ (viewed as a subspace of \mathbb{R}^d) is:*

$$\mathbf{P}_{\mathbf{x}} := (\mathbf{I}_n - (\mathbf{x}^{\mathbf{T}} \mathbf{B} \mathbf{M}^{-1} \mathbf{B} \mathbf{x})^{-1} \mathbf{M}^{-1} \mathbf{B} \mathbf{x} \mathbf{x}^{\mathbf{T}} \mathbf{B}). \quad (6)$$

Next, we consider the $\text{grad} \bar{f}(\mathbf{x})$. Note that it is *not* the Euclidean gradient $\nabla \bar{f}(\mathbf{x})$, even though \bar{f} is defined on \mathbb{R}^d . The reason is that \bar{f} is defined on a \mathbb{R}^d endowed with a non-standard inner product. According to Eq. (3.31) from (Absil et al., 2009), we have

$$\text{grad} \bar{f}(\mathbf{x})^{\mathbf{T}} \mathbf{M} \xi_{\mathbf{x}} = D\bar{f}(\mathbf{x})[\xi_{\mathbf{x}}] = \nabla \bar{f}(\mathbf{x})^{\mathbf{T}} \bar{\xi}_{\mathbf{x}}$$

for every $\bar{\xi}_{\mathbf{x}} \in \mathbb{R}^d$ ($Df(\mathbf{x})$ denotes the *differential* of f at \mathbf{x}), so $\text{grad} \bar{f}(\mathbf{x}) = \mathbf{M}^{-1} \nabla \bar{f}(\mathbf{x})$. Thus, we have

$$\text{grad} f(\mathbf{x}) = \mathbf{P}_{\mathbf{x}} \mathbf{M}^{-1} \nabla \bar{f}(\mathbf{x}). \quad (7)$$

Riemannian Hessian. The Riemannian Hessian of a given function f can be computed in ambient coordinates via the formula:

$$\begin{aligned} \text{Hess} f(\mathbf{x})[\eta_{\mathbf{x}}] &= \mathbf{P}_{\mathbf{x}} \mathbf{M}^{-1} \nabla^2 \bar{f}(\mathbf{x}) \eta_{\mathbf{x}} - \mathbf{P}_{\mathbf{x}} ((\mathbf{x}^{\mathbf{T}} \mathbf{M} \mathbf{P}_{\mathbf{x}}^{\perp} \mathbf{M}^{-1} \nabla \bar{f}(\mathbf{x})) \mathbf{M}^{-1} \mathbf{B}) \eta_{\mathbf{x}} \\ &= \mathbf{P}_{\mathbf{x}} \mathbf{M}^{-1} [\nabla^2 \bar{f}(\mathbf{x}) - (\mathbf{x}^{\mathbf{T}} \nabla \bar{f}(\mathbf{x}) - g_{\mathbf{x}}(\mathbf{x}, \text{grad} f(\mathbf{x}))) \mathbf{B}] \eta_{\mathbf{x}}. \end{aligned} \quad (8)$$

The derivation is rather elaborate, so due to space constraints we defer it to Appendix B.

4. Metric Selection Matters

Our proposed algorithms for CCA and LDA are based on using a preconditioner to define the Riemannian metric. Before proceeding, in order to motivate our strategy, we give two simple examples that illustrate that in the context of Riemannian optimization with quadratic equality constraints, the metric selection can have a substantial effect on the convergence speed of the optimization.

Example 1 (Linear Objective) *Let us consider the following problem*

$$\max_{\mathbf{x} \in \mathbb{R}^d} \mathbf{b}^T \mathbf{x} \quad \text{s.t.} \quad \mathbf{x}^T \mathbf{B} \mathbf{x} = 1 \quad (9)$$

for some vector $\mathbf{b} \in \mathbb{R}^d$. The solution is $\mathbf{x}^* = \mathbf{B}^{-1} \mathbf{b} / \|\mathbf{B}^{-1} \mathbf{b}\|_{\mathbf{B}}$.

The Euclidean gradient is simply \mathbf{b} , independent of \mathbf{x} . Plugging it to Eq. (7), using Eq. (4), and plugging both to Eq. (2) leads us to the iteration

$$\begin{aligned} \mathbf{y}_{k+1} &= \mathbf{x}_k + \tau_k \left(\mathbf{M}^{-1} \mathbf{b} - \frac{\mathbf{x}_k^T \mathbf{B} \mathbf{M}^{-1} \mathbf{b}}{\mathbf{x}_k^T \mathbf{B} \mathbf{M}^{-1} \mathbf{B} \mathbf{x}_k} \mathbf{M}^{-1} \mathbf{B} \mathbf{x}_k \right) \\ \mathbf{x}_{k+1} &= \frac{\mathbf{y}_{k+1}}{\|\mathbf{y}_{k+1}\|_{\mathbf{B}}} . \end{aligned}$$

We see, as expected, that the iterations depend on the choice of the Riemannian metric defined by the matrix \mathbf{M} . If we use the metric $\mathbf{M} = \mathbf{B}$, and take $\tau_0 = 1/\mathbf{x}_0^T \mathbf{b}$, the iteration reduces to $\mathbf{x}_1 = \mathbf{B}^{-1} \mathbf{b} / \|\mathbf{B}^{-1} \mathbf{b}\|_{\mathbf{B}}$, i.e. the problem is solved in a single iteration.

Example 2 (Inverse Power Iteration) *Consider maximizing $\mathbf{x}^T \mathbf{x}$ subject to $\mathbf{x}^T \mathbf{A} \mathbf{x} = 1$, where \mathbf{A} is a SPD matrix. The solution is equal the eigenvector corresponding the smallest eigenvalue of \mathbf{A} (which is also the eigenvector corresponding to the maximum eigenvalue of \mathbf{A}^{-1}). If we use gradient ascent on $\mathbb{S}^{\mathbf{A}}$ with metric selection $g_{\mathbf{x}}(\xi_{\mathbf{x}}, \eta_{\mathbf{x}}) = \xi_{\mathbf{x}}^T \mathbf{A} \eta_{\mathbf{x}}$ (in ambient coordinates), and chose step sizes $\tau_k = (\mathbf{x}_k^T \mathbf{x}_k)^{-1}$, then the iteration reduces to $\mathbf{x}_{k+1} = \mathbf{A}^{-1} \mathbf{x}_k / \|\mathbf{A}^{-1} \mathbf{x}_k\|_2$, i.e. inverse power method, which is well known for it good convergence properties.*

5. Iterative Methods for CCA and LDA

In this section we present novel preconditioned algorithms for CCA and LDA. At the core, the algorithms use Riemannian optimization, where the constraints, which are quadratic equality constraints, are treated as a Riemannian manifold, according to the geometry defined in Section 3. Preconditioning is incorporated by choosing the Riemannian metric.

To understand the effect of the preconditioner, we analyze the condition number of the Riemannian Hessian at the optimum, when viewed as a linear operator on the tangent space. The analysis is well motivated by the literature, see (Absil et al., 2009, Theorem 4.5.6, Theorem 7.4.11 and Equation 7.5), though the results are, unfortunately, only asymptotic.

Additionally, we use the bounds to derive a notion of optimal preconditioner. As expected, the optimal preconditioner is too expensive to compute, but identifying it serves as a guideline for designing preconditioners (and our results allow us to reason about their quality).

5.1. Canonical Correlation Analysis

CCA, originally introduced by [Hotelling \(1936\)](#), is a well-established method in statistical learning with numerous applications (e.g. [\(Sun et al., 2010; Chaudhuri et al., 2009; Dhillon et al., 2011, 2012; Su et al., 2012; Kim et al., 2007\)](#)). In CCA the relation between a pair of datasets in matrix form is analyzed, where the goal is to find the directions of maximal correlation between a pair of observed variables. In the language of linear algebra, CCA measures the similarities between two subspaces spanned by the columns of the two matrices.

In this paper, we consider a regularized version of CCA defined below²:

Definition 4 Let $\mathbf{X} \in \mathbb{R}^{n \times d_x}$ and $\mathbf{Y} \in \mathbb{R}^{n \times d_y}$ be two data matrices, and $\lambda_x, \lambda_y \geq 0$ be two regularization parameter. Let $q = \max(\text{rank}(\mathbf{X}^T \mathbf{X} + \lambda_x \mathbf{I}_{d_x}), \text{rank}(\mathbf{Y}^T \mathbf{Y} + \lambda_y \mathbf{I}_{d_y}))$. The (λ_x, λ_y) canonical correlations $\sigma_1 \geq \dots \geq \sigma_q$ and the (λ_x, λ_y) canonical weights $\mathbf{u}_1, \dots, \mathbf{u}_q, \mathbf{v}_1, \dots, \mathbf{v}_q$ are the ones that maximize

$$\text{Tr}(\mathbf{U}^T \mathbf{X}^T \mathbf{Y} \mathbf{V})$$

subject to

$$\mathbf{U}^T(\mathbf{X}^T \mathbf{X} + \lambda_x \mathbf{I}_{d_x})\mathbf{U} = \mathbf{I}_{d_x}, \quad \mathbf{V}^T(\mathbf{Y}^T \mathbf{Y} + \lambda_y \mathbf{I}_{d_y})\mathbf{V} = \mathbf{I}_{d_y}$$

where $\mathbf{U}^T \mathbf{X}^T \mathbf{Y} \mathbf{V} = \text{diag}(\sigma_1, \dots, \sigma_q)$, $\mathbf{U} = [\mathbf{u}_1 \dots \mathbf{u}_q]$ and $\mathbf{V} = [\mathbf{v}_1 \dots \mathbf{v}_q]$.

In his paper, we focus on finding the top correlation, i.e. finding σ_1, \mathbf{u}_1 and \mathbf{v}_1 . Trailing correlations and weights can be obtained by deflating the original problem.

It is useful to introduce the following notation:

$$\Sigma_{xx} = \mathbf{X}^T \mathbf{X} + \lambda_x \mathbf{I}_{d_x}, \Sigma_{yy} = \mathbf{Y}^T \mathbf{Y} + \lambda_y \mathbf{I}_{d_y}, \Sigma_{xy} = \mathbf{X}^T \mathbf{Y}.$$

With these notations, the problem of finding \mathbf{u}_1 and \mathbf{v}_1 can be succinctly formulated as the solution of the following optimization problem:

$$\max \mathbf{u}^T \Sigma_{xy} \mathbf{v} \quad \text{s.t.} \quad \mathbf{u} \in \mathbb{S}^{\Sigma_{xx}}, \mathbf{v} \in \mathbb{S}^{\Sigma_{yy}}$$

The optimal solution is ([Bjorck and Golub, 1973](#))

$$\mathbf{u}_1 = \Sigma_{xx}^{-\frac{1}{2}} \tilde{\mathbf{u}}_1 \quad \mathbf{v}_1 = \Sigma_{yy}^{-\frac{1}{2}} \tilde{\mathbf{v}}_1 \tag{10}$$

where $\tilde{\mathbf{u}}_1$ and $\tilde{\mathbf{v}}_1$ are the left and right unit-length singular vector corresponding to the largest singular value σ_1 of the matrix

$$\mathbf{R} = \Sigma_{xx}^{-\frac{1}{2}} \Sigma_{xy} \Sigma_{yy}^{-\frac{1}{2}}. \tag{11}$$

5.1.1. PRECONDITIONED CCA ALGORITHM

Finding the leading correlation is a case of minimization on a Riemannian manifold: the constraint set is the product manifold $\mathbb{S}_{xy} := \mathbb{S}^{\Sigma_{xx}} \times \mathbb{S}^{\Sigma_{yy}}$, and the objective is $f(\mathbf{u}, \mathbf{v}) = -\mathbf{u}^T \Sigma_{xy} \mathbf{v}$. Thus, we consider the use of Riemannian optimization to solve this problem, while exploiting the geometry developed in Section 3 (however, since we have two manifold constraints, we need to use a product manifold as described in Appendix C). We use some SPD matrices \mathbf{M}_{xx} and \mathbf{M}_{yy} to

2. The definition is formulated as a linear algebra problem. While the problem can be motivated, and described, in the language of statistics, the linear algebraic formulation is more convenient for our purposes.

define Riemannian metrics on $\mathbb{S}^{\Sigma_{xx}}$ and $\mathbb{S}^{\Sigma_{yy}}$ (respectively), and these, in turn, define a Riemannian metric on \mathbb{S}_{xy} .

Denote $d = d_x + d_y$ and $\mathbf{z} = \begin{bmatrix} \mathbf{u} \\ \mathbf{v} \end{bmatrix} \in \mathbb{R}^d$ where $\mathbf{u} \in \mathbb{R}^{d_x}$ and $\mathbf{v} \in \mathbb{R}^{d_y}$. We will abuse notation and view \mathbb{S}_{xy} as a subset of \mathbb{R}^d given by this coordinate split. With this convention, the objective function to be minimized can be rewritten as

$$f(\mathbf{z}) = -\frac{1}{2}\mathbf{z}^T \begin{bmatrix} 0 & \Sigma_{xy} \\ \Sigma_{xy}^T & 0 \end{bmatrix} \mathbf{z}. \quad (12)$$

As usual, let \bar{f} denote the extension of f to \mathbb{R}^d , given by the same formula. For $\mathbf{u} \in \mathbb{S}^{\Sigma_{xx}}$, let \mathbf{P}_u denote the projection on $T_u \mathbb{S}^{\Sigma_{xx}}$ (Eq. (6)), and similarly for \mathbf{P}_v where $\mathbf{v} \in \mathbb{S}^{\Sigma_{yy}}$. For $\mathbf{z} \in \mathbb{S}_{xy}$ let $\mathbf{P}_z = \text{diag}(\mathbf{P}_u, \mathbf{P}_v)$. The Riemannian metric on $\mathbb{S}^{\Sigma_{xx}} \times \mathbb{S}^{\Sigma_{yy}}$ is defined by the SPD matrix $\mathbf{M} = \text{diag}(\mathbf{M}_{xx}, \mathbf{M}_{yy})$. The following are analytical expressions for the Riemannian gradient and the Riemannian Hessian in ambient coordinates:

$$\text{grad} f(\mathbf{z}) = \mathbf{P}_z \mathbf{M}^{-1} \nabla \bar{f}(\mathbf{z}) = - \begin{bmatrix} \mathbf{P}_u \mathbf{M}_{xx}^{-1} \Sigma_{xy} \mathbf{v} \\ \mathbf{P}_v \mathbf{M}_{yy}^{-1} \Sigma_{xy}^T \mathbf{u} \end{bmatrix} \quad (13)$$

$$\text{Hess} f(\mathbf{z})[\eta_z] = \mathbf{P}_z \mathbf{M}^{-1} \begin{bmatrix} (\mathbf{u}^T \mathbf{M}_{xx} \mathbf{P}_u^\perp \mathbf{M}_{xx}^{-1} \Sigma_{xy} \mathbf{v}) \cdot \Sigma_{xx} & -\Sigma_{xy} \\ -\Sigma_{xy}^T & (\mathbf{v}^T \mathbf{M}_{yy} \mathbf{P}_v^\perp \mathbf{M}_{yy}^{-1} \Sigma_{xy}^T \mathbf{u}) \cdot \Sigma_{yy} \end{bmatrix} \eta_z \quad (14)$$

Along with formulas for the retraction and vector transport, these can be used in any Riemannian optimization algorithm.

5.1.2. COMPLEXITY AND CONDITION NUMBER

The following is our main theoretical result regarding our preconditioned CCA algorithm. It shows that, as expected for a preconditioned iterative method, if we have a factorization of the preconditioner then each iteration is cheap. Furthermore, it bounds the relevant condition based on how well the preconditioner approximates a specific matrix ($\Sigma := \text{diag}(\Sigma_{xx}, \Sigma_{yy})$).

Theorem 5 *Assume $n \geq \max(d_x, d_y)$, and that both $\text{nnz}(\mathbf{X})$ and $\text{nnz}(\mathbf{Y})$ are at least n . Consider using Riemannian optimization to minimize $-\mathbf{u}^T \Sigma_{xy} \mathbf{v}$ subject to $\mathbf{u} \in \mathbb{S}^{\Sigma_{xx}}$ and $\mathbf{v} \in \mathbb{S}^{\Sigma_{yy}}$, where we use the Riemannian metric defined by $\mathbf{M} = \text{diag}(\mathbf{M}_{xx}, \mathbf{M}_{yy})$ where $\mathbf{M}_{xx} \in \mathbb{R}^{d_x \times d_x}$ and $\mathbf{M}_{yy} \in \mathbb{R}^{d_y \times d_y}$ are given preconditioners matrices. Denote by $T_{\mathbf{M}}$ and $T_{\mathbf{M}^{-1}}$ the cost (number of operations) of computing the product of \mathbf{M} and \mathbf{M}^{-1} (respectively) with a vector (potentially, after preprocessing \mathbf{M}). Then, assuming all computations are done in ambient \mathbb{R}^d coordinates: function evaluation, vector transport and retraction costs $O(\text{nnz}(\mathbf{X}) + \text{nnz}(\mathbf{Y}))$, gradient computation costs $O(\text{nnz}(\mathbf{X}) + \text{nnz}(\mathbf{Y}) + T_{\mathbf{M}^{-1}})$, and applying the Hessian to a vector takes $O(\text{nnz}(\mathbf{X}) + \text{nnz}(\mathbf{Y}) + T_{\mathbf{M}^{-1}} + T_{\mathbf{M}})$. Furthermore, assuming $\sigma_1 - \sigma_2 > 0$ and that Σ is a SPD matrix, the condition number of the Riemannian Hessian at the optimum is at most $\frac{2\sigma_1}{\sigma_1 - \sigma_2} \cdot \kappa(\Sigma, \mathbf{M})$ where $\Sigma = \text{diag}(\Sigma_{xx}, \Sigma_{yy})$.*

The condition number bound decomposes to two components: the first is the relative eigengap ($2\sigma_1/(\sigma_1 - \sigma_2)$), which forms a natural condition number for the problem (if the first and second correlations are very close, it is very hard to distinguish between them) that almost always appears in problems of this form, and a second component which measures how close the preconditioner-defined metric approximates the natural metric for the constraints. The optimal preconditioner,

according to the bound, is $\mathbf{M} = \Sigma$. However, using this preconditioner, requires explicitly computing it in $O(nd^2)$ time. This is too expensive, since the exact correlations can be computed analytically in $O(nd^2)$ time as well (Bjorck and Golub, 1973).

5.2. Linear Discriminant Analysis

LDA, introduced by Fisher (1936), is a well-known method for classification (Mika et al., 1999), and more commonly for dimension reduction before classification (Chen et al., 2012). The latter is achieved by finding an embedding such that the between-class scatter is maximized and the within-class scatter is minimized simultaneously.

In this paper, we consider a regularized version of LDA as defined below:

Definition 6 (Section 4.3.3 in Friedman et al. (2001)). Let $\chi_1 = \{\mathbf{x}_1^1, \dots, \mathbf{x}_{n_1}^1\}, \dots, \chi_m = \{\mathbf{x}_1^l, \dots, \mathbf{x}_{n_m}^l\} \subseteq \mathbb{R}^d$ be samples from l different classes, and denote $\chi = \chi_1 \cup \dots \cup \chi_m = \{\mathbf{x}_1, \dots, \mathbf{x}_n\}$. Let $\{y_1, \dots, y_n\}$ be the corresponding labels. Let \mathbf{m}_k , for $k = 1, \dots, l$, denote the sample mean of class k (i.e., $\mathbf{m}_k = \frac{1}{n_k} \sum_{i=1}^{n_k} \mathbf{x}_i^k \in \mathbb{R}^d$), and \mathbf{m} denote the dataset sample mean. Let \mathbf{S}_B and \mathbf{S}_w be the between-class and within-class covariance matrices:

$$\mathbf{S}_B := \sum_{k=1}^l n_k (\mathbf{m}_k - \mathbf{m})(\mathbf{m}_k - \mathbf{m})^T \quad \mathbf{S}_w := \sum_{i=1}^n (\mathbf{x}_i - \mathbf{m}_{y_i})(\mathbf{x}_i - \mathbf{m}_{y_i})^T$$

Let $\lambda \geq 0$ be a regularization parameter. The j th discriminant variable \mathbf{w}_j is a maximizer of the generalized Rayleigh quotient

$$J(\mathbf{w}) = \frac{\mathbf{w}^T \mathbf{S}_B \mathbf{w}}{\mathbf{w}^T (\mathbf{S}_w + \lambda \mathbf{I}_d) \mathbf{w}}, \quad (15)$$

subject to $\mathbf{w}_j \perp \mathbf{w}_1, \dots, \mathbf{w}_j \perp \mathbf{w}_{j-1}$. Note that these are the eigenvectors of $(\mathbf{S}_B, \mathbf{S}_w + \lambda \mathbf{I})$.

In his paper, we focus on finding the leading discriminant variable. This vector is the solution of the optimization problem of maximizing $\mathbf{w}^T \mathbf{S}_B \mathbf{w}$ subject to $\mathbf{w}^T (\mathbf{S}_w + \lambda \mathbf{I}_d) \mathbf{w} = 1$. Trailing discriminant variables can be obtained by deflating the original problem.

Denote the optimal solution $\mathbf{w}^* = \mathbf{w}_1$ and denote the eigenvalues of the matrix pencil $(\mathbf{S}_B, \mathbf{S}_w + \lambda \mathbf{I}_d)$ by $\rho_1 \geq \rho_2 \geq \dots \geq \rho_d \geq 0$. For purpose of describing and analyzing our algorithm, it is useful to write,

$$\mathbf{S}_w = \hat{\mathbf{X}}^T \hat{\mathbf{X}}, \quad \hat{\mathbf{X}} := \mathbf{X} - \mathbf{Y}, \quad \mathbf{S}_B = \hat{\mathbf{Y}}^T \hat{\mathbf{Y}},$$

where $\hat{\mathbf{X}} \in \mathbb{R}^{n \times d}$ is a matrix such that each i -th row of $\hat{\mathbf{X}}$ is $(\mathbf{x}_i - \mathbf{m}_{y_i})^T$, $\mathbf{X} \in \mathbb{R}^{n \times d}$ is a matrix such that each i -th row of \mathbf{X} is \mathbf{x}_i^T , $\mathbf{Y} \in \mathbb{R}^{n \times d}$ is a matrix such that each i -th row is of the form \mathbf{m}_{y_i} , and $\hat{\mathbf{Y}} \in \mathbb{R}^{l \times d}$ is a matrix such that each k -th row of $\hat{\mathbf{Y}}$ is $\sqrt{n_k}(\mathbf{m}_k - \mathbf{m})^T$.

5.2.1. PRECONDITIONED LDA ALGORITHM

Finding the leading discriminant variable is a case of minimization on a Riemannian manifold: the constraint set is $\mathbb{S}^{\mathbf{S}_w + \lambda \mathbf{I}_d}$, and the objective is $f(\mathbf{w}) = -\frac{1}{2} \mathbf{w}^T \mathbf{S}_B \mathbf{w}$. Thus, like in the previous subsection, we consider the use of Riemannian optimization to solve this problem, while exploiting the geometry developed in Section 3. As before, we use some SPD matrix $\mathbf{M} \in \mathbb{R}^{d \times d}$ to define Riemannian metric on $\mathbb{S}^{\mathbf{S}_w + \lambda \mathbf{I}_d}$.

The Riemannian optimization components are computed as in Section 3. Let \bar{f} be the extension of f to \mathbb{R}^d given by the same formula. For $\mathbf{w} \in \mathbb{S}^{\mathbf{S}_w + \lambda \mathbf{I}_d}$, let \mathbf{P}_w denote the projection on

$T_{\mathbf{w}}\mathbb{S}^{\mathbf{S}_{\mathbf{w}}+\lambda\mathbf{I}_d}$ (Eq. (6)). The following are analytical expressions for the Riemannian gradient and the Riemannian Hessian in ambient coordinates:

$$\mathbf{grad}f(\mathbf{w}) = -\mathbf{P}_{\mathbf{w}}\mathbf{M}^{-1}\mathbf{S}_{\mathbf{B}}\mathbf{w}, \quad (16)$$

$$\mathbf{Hess}f(\mathbf{w})[\eta_{\mathbf{w}}] = \mathbf{P}_{\mathbf{w}}\mathbf{M}^{-1}[-\mathbf{S}_{\mathbf{B}} + (\mathbf{w}^T\mathbf{S}_{\mathbf{B}}\mathbf{w} - g_{\mathbf{w}}(\mathbf{w}, \mathbf{grad}f(\mathbf{w}))) (\mathbf{S}_{\mathbf{w}} + \lambda\mathbf{I}_d)] \eta_{\mathbf{w}}. \quad (17)$$

Along with formulas for the retraction and vector transport, these can be used in any Riemannian optimization algorithm.

5.2.2. COMPLEXITY AND CONDITION NUMBER

Similarly to the CCA, the following is our main theoretical result regarding our preconditioned LDA algorithm. It shows that, as expected for a preconditioned iterative method, if we have a factorization of the preconditioner then each iteration is cheap. Furthermore, it bounds the relevant condition based on how well the preconditioner approximates a specific matrix ($\mathbf{S}_{\mathbf{w}} + \lambda\mathbf{I}_d$).

Theorem 7 *Assume $n \geq d$, and that $\mathbf{nnz}(\mathbf{X}) \geq ld$. Consider using Riemannian optimization to minimize $-\mathbf{w}^T\mathbf{S}_{\mathbf{B}}\mathbf{w}$ subject to $\mathbf{w} \in \mathbb{S}^{\mathbf{S}_{\mathbf{w}}+\lambda\mathbf{I}_d}$, where we use the Riemannian metric defined by $\mathbf{M} \in \mathbb{R}^{d \times d}$, which is a given preconditioner matrix. Denote by $T_{\mathbf{M}}$ and $T_{\mathbf{M}^{-1}}$ the cost (number of operations) of computing the product of \mathbf{M} and \mathbf{M}^{-1} (respectively) with a vector (potentially, after preprocessing \mathbf{M}). Then, assuming all computations are done in ambient \mathbb{R}^d coordinates: function evaluation costs $O(ld)$, vector transport and retraction costs $O(\mathbf{nnz}(\mathbf{X}))$, gradient computation costs $O(\mathbf{nnz}(\mathbf{X}) + T_{\mathbf{M}^{-1}})$, and applying the Hessian to a vector takes $O(\mathbf{nnz}(\mathbf{X}) + T_{\mathbf{M}^{-1}} + T_{\mathbf{M}})$. Furthermore, assuming $\rho_1 - \rho_2 > 0$, $\rho_d = 0^3$ and that $\mathbf{S}_{\mathbf{w}} + \lambda\mathbf{I}_d$ is non-singular, the condition number of the Riemannian Hessian at the optimum is at most $\frac{\rho_1}{\rho_1 - \rho_2} \cdot \kappa(\mathbf{S}_{\mathbf{w}} + \lambda\mathbf{I}_d, \mathbf{M})$.*

The condition number bound decomposes to two components: the first is the relative eigengap ($\rho_1/(\rho_1 - \rho_2)$), which form a natural condition number for the problem (if the first and second generalized eigenvalues are very close, it is very hard to distinguish between invariant subspaces corresponding to them) that almost always appears in problems of this form, and a second component which measures how close the preconditioner-defined metric approximates the natural metric for the constraints. The optimal preconditioner, according to the bound, is $\mathbf{M} = \mathbf{S}_{\mathbf{w}} + \lambda\mathbf{I}_d$. However, using this preconditioner, requires explicitly computing it in $O(nd^2)$ time. This is too expensive, since the exact discriminant variables can be computed analytically in $O(nd^2)$ time as well (exact solution requires finding the inverse of $\mathbf{S}_{\mathbf{w}} + \lambda\mathbf{I}_d$ and then finding the first eigenvalue and corresponding eigenvector of $(\mathbf{S}_{\mathbf{w}} + \lambda\mathbf{I}_d)^{-1}\mathbf{S}_{\mathbf{B}}$).

6. Randomized Riemannian Preconditioning

In the previous section we described generic preconditioned methods. In this section we show how to use sketching to form an effective preconditioner. Our sketching-based preconditioning strategy is well developed in the literature, and we merely explain how it is applicable for our case.

For CCA and LDA the preconditioner needs to approximate regularized Gram matrices. For CCA, the preconditioners $\mathbf{M}_{\mathbf{x}}$ and $\mathbf{M}_{\mathbf{y}}$ should approximate $\Sigma_{\mathbf{xx}} = \mathbf{X}^T\mathbf{X} + \lambda_{\mathbf{x}}\mathbf{I}$ and $\Sigma_{\mathbf{yy}} = \mathbf{Y}^T\mathbf{Y} + \lambda_{\mathbf{y}}\mathbf{I}$ (respectively). For LDA, the preconditioner \mathbf{M} should approximate $\mathbf{S}_{\mathbf{w}} + \lambda\mathbf{I}_d = \hat{\mathbf{X}}^T\hat{\mathbf{X}}$.

3. This usually the case since the number of labels is much smaller than the number of samples.

Since computing various components required for Riemannian optimization (e.g., Riemannian gradient) requires the application of the inverse of the preconditioner, an implicit representation of the preconditioner is not sufficient, and a factorization (or some other representation that allows efficient inverse application) is needed. Obviously, for both CCA and LDA the relevant Gram matrices can be computed in $O(nd^2)$ time where d is the data dimension ($\max(d_x, d_y)$ for CCA). However, this is as expensive as solving the problem exactly. Thus, our goal is to describe strategies that compute provably good approximations to Gram matrices in $o(nd^2)$ time.

Let \mathbf{Z} be a generic data matrix of size $n \times d$, and let $\lambda \geq 0$ be a generic regularization parameter. Our strategy for approximating $\mathbf{Z}^T \mathbf{Z} + \lambda \mathbf{I}$ is to compute the product $\mathbf{Z}^T \mathbf{S}^T \mathbf{S} \mathbf{Z} + \lambda \mathbf{I}$ where $\mathbf{S} \in \mathbb{R}^{s \times n}$. Once $\mathbf{S} \mathbf{Z}$ is computed, it is possible to compute $\mathbf{Z}^T \mathbf{S}^T \mathbf{S} \mathbf{Z} + \lambda \mathbf{I}$ in $O(sd^2)$ ⁴, so our goal is to design sketching matrices \mathbf{S} such that $\mathbf{S} \mathbf{Z}$ is cheap to compute, and $\kappa(\mathbf{Z}^T \mathbf{Z} + \lambda \mathbf{I}, \mathbf{Z}^T \mathbf{S}^T \mathbf{S} \mathbf{Z} + \lambda \mathbf{I})$ is bounded by a constant. There are quite a few distributions developed in the literature from which \mathbf{S} can be sampled. For concreteness, we describe the use of the COUNTSKETCH transformation (Charikar et al., 2004; Clarkson and Woodruff, 2017), although Subsampled Randomized Hadamard Transform is also a good choice, in particular for dense datasets. COUNTSKETCH is specified by a random hash function $h : \{1, \dots, d\} \rightarrow \{1, \dots, s\}$ and random sign function $g : \{1, \dots, d\} \rightarrow \{-1, +1\}$. Applying \mathbf{S} to a vector \mathbf{x} is given by the formula $(\mathbf{S} \mathbf{x})_i = \sum_{j|h(j)=i} g(j)x_j$. It is easy to see that \mathbf{S} is a random matrix in which the j th column contains a single nonzero entry $g(j)$ in the $h(j)$ th row. Clearly, $\mathbf{S} \mathbf{Z}$ can be computed in $\text{nnz}(\mathbf{Z}) = O(nd)$ time. Thus, it only remains to bound the condition number. The following lemma shows that if the sketch size is large enough, then with high probability the condition number is bounded by a constant.

Lemma 8 *Assume that $\lambda > 0$ or that $\mathbf{Z} \in \mathbb{R}^{n \times d}$ has full column rank. Let $s_\lambda(\mathbf{Z}) := \text{Tr}((\mathbf{Z}^T \mathbf{Z} + \lambda \mathbf{I})^{-1} \mathbf{Z}^T \mathbf{Z})$. Suppose that \mathbf{S} is a COUNTSKETCH matrix with $s \geq 20s_\lambda(\mathbf{Z})^2/\delta$ for some $\delta \in (0, 1)$. Then with probability of at least $1 - \delta$ we have $\kappa(\mathbf{Z}^T \mathbf{Z} + \lambda \mathbf{I}, \mathbf{Z}^T \mathbf{S}^T \mathbf{S} \mathbf{Z} + \lambda \mathbf{I}) \leq 3$.*

The last lemma justifies the use of COUNTSKETCH to form the preconditioner. Furthermore, our sketching-based preconditioner construction naturally allows for a warm-start. While this is not captured by our theory, heuristically (and empirically) the Riemannian optimization part of our proposed algorithm converges faster if the starting vectors are close to the optimum. Our sketching approach lets us quickly compute good starting vectors. For CCA, after computing $\mathbf{S} \mathbf{X}$ and $\mathbf{S} \mathbf{Y}$, we can compute the leading canonical weights $\tilde{\mathbf{u}}$ and $\tilde{\mathbf{v}}$ of $(\mathbf{S} \mathbf{X}, \mathbf{S} \mathbf{Y})$, normalize them (i.e., compute $\tilde{\mathbf{u}}/\|\tilde{\mathbf{u}}\|_{\Sigma_{\mathbf{X}\mathbf{X}}}$ and $\tilde{\mathbf{v}}/\|\tilde{\mathbf{v}}\|_{\Sigma_{\mathbf{Y}\mathbf{Y}}}$), and use these as starting vectors. For LDA, after computing $\mathbf{M} = \hat{\mathbf{X}}^T \mathbf{S}^T \mathbf{S} \hat{\mathbf{X}}$ we can compute the leading eigenvector $\tilde{\mathbf{w}}$ of $(\mathbf{S}_B, \mathbf{M})$, normalize it (i.e., compute $\tilde{\mathbf{w}}/\|\tilde{\mathbf{w}}\|_{\mathbf{S}_w + \lambda \mathbf{I}}$), and use it as a starting vector.

A pseudo code description appears in the Appendix in Algorithms 1 and 2. The following two corollaries summarize our theoretical results regarding the proposed algorithms. These corollaries follow almost immediately from the previous theorems, so we omit the proof. We remark that COUNTSKETCH can possibly be replaced with other sketching transforms (such as Subsampled Randomized Hadamard Transform), and Riemannian CG can be replaced with other Riemannian optimization methods.

4. We remark that for numerical stability, it might be better actually use a QR factorization of $\begin{bmatrix} \mathbf{S} \mathbf{Z} \\ \sqrt{\lambda} \mathbf{I} \end{bmatrix}$ instead.

Corollary 9 Consider Algorithm 1. Let $\delta \in (0, 1)$ and denote $d = \max(d_x, d_y)$ and $s_\lambda = \max(s_{\lambda_x}(\mathbf{X}), s_{\lambda_x}(\mathbf{Y}))$. If $s = \lceil 40s_\lambda^2/\delta \rceil$, then with probability of at least $1 - \delta$, for Riemannian CG, the condition number of the Riemannian Hessian at the optimum is bounded by $6\sigma_1/(\sigma_1 - \sigma_2)$ regardless of the condition number of Σ_{xx} and Σ_{yy} . Furthermore, assuming $\text{nnz}(\mathbf{X}) \geq n$ and $\text{nnz}(\mathbf{Y}) \geq n$, the preprocessing steps takes $o(\text{nnz}(\mathbf{X}) + \text{nnz}(\mathbf{Y}) + \text{poly}(d))$, and each iteration takes $O(\text{nnz}(\mathbf{X}) + \text{nnz}(\mathbf{Y}) + d^2)$.

Corollary 10 Consider Algorithm 2. Let $\delta \in (0, 1)$. If $s = \lceil 20s_\lambda(\hat{\mathbf{X}})^2/\delta \rceil$, then with probability of at least $1 - \delta$, for Riemannian CG, the condition number of the Hessian at the optimum is bounded by $3\rho_1/(\rho_1 - \rho_2)$ regardless of the condition number of $\mathbf{S}_w + \lambda\mathbf{I}$. Furthermore, the preprocessing steps takes $O(\text{nnz}(\mathbf{X}) + ld + \text{poly}(d))$, and each iteration takes $O(\text{nnz}(\mathbf{X}) + (l + d)d)$.

Acknowledgments

The authors thanks Bart Vandereycken for useful discussions. This research was supported by the Israel Science Foundation (grant no. 1272/17).

References

- P. A. Absil, R. Mahony, and R. Sepulchre. *Optimization Algorithms on Matrix Manifolds*. Princeton University Press, 2009. ISBN 978-0-6911-3298-3.
- P. A. Absil, R. Mahony, and J. Trumpf. An Extrinsic Look at the Riemannian Hessian. In *Geometric Science of Information*, pages 361–368. Springer, 2013.
- Haim Avron, Petar Maymounkov, and Sivan Toledo. Blendenpik: Supercharging LAPACK’s least-squares solver. *SIAM Journal on Scientific Computing*, 32(3):1217–1236, 2010.
- Haim Avron, Christos Boutsidis, Sivan Toledo, and Anastasios Zouzias. Efficient dimensionality reduction for canonical correlation analysis. *SIAM Journal on Scientific Computing*, 36(5):S111–S131, 2014a. doi: 10.1137/130919222. URL <http://dx.doi.org/10.1137/130919222>.
- Haim Avron, Huy Nguyen, and David Woodruff. Subspace embeddings for the polynomial kernel. In Z. Ghahramani, M. Welling, C. Cortes, N. D. Lawrence, and K. Q. Weinberger, editors, *Advances in Neural Information Processing Systems 27*, pages 2258–2266. Curran Associates, Inc., 2014b. URL <http://papers.nips.cc/paper/5240-subspace-embeddings-for-the-polynomial-kernel>
- Haim Avron, Kenneth L. Clarkson, and David P. Woodruff. Sharper Bounds for Regularized Data Fitting. In Klaus Jansen, José D. P. Rolim, David Williamson, and Santosh S. Vempala, editors, *Approximation, Randomization, and Combinatorial Optimization. Algorithms and Techniques (APPROX/RANDOM 2017)*, volume 81 of *Leibniz International Proceedings in Informatics (LIPIcs)*, pages 27:1–27:22, Dagstuhl, Germany, 2017. Schloss Dagstuhl–Leibniz-Zentrum fuer Informatik. ISBN 978-3-95977-044-6. doi: 10.4230/LIPIcs.APPROX-RANDOM.2017.27. URL <http://drops.dagstuhl.de/opus/volltexte/2017/7576>.

- Ake Bjorck and Gene H Golub. Numerical methods for computing angles between linear subspaces. *Mathematics of Computation*, 27(123):579–594, 1973.
- N. Boumal, B. Mishra, P.-A. Absil, and R. Sepulchre. Manopt, a Matlab toolbox for optimization on manifolds. *Journal of Machine Learning Research*, 15:1455–1459, 2014. URL <http://www.manopt.org>.
- Moses Charikar, Kevin Chen, and Martin Farach-Colton. Finding frequent items in data streams. *Theoretical Computer Science*, 312(1):3 – 15, 2004. ISSN 0304-3975. doi: [https://doi.org/10.1016/S0304-3975\(03\)00400-6](https://doi.org/10.1016/S0304-3975(03)00400-6). URL <http://www.sciencedirect.com/science/article/pii/S0304397503004006>. Automata, Languages and Programming.
- Kamalika Chaudhuri, Sham M Kakade, Karen Livescu, and Karthik Sridharan. Multi-view clustering via canonical correlation analysis. In *Proceedings of the 26th annual International Conference on Machine Learning (ICML)*, pages 129–136. ACM, 2009.
- Minhua Chen, William Carson, Miguel Rodrigues, Robert Calderbank, and Lawrence Carin. Communications inspired linear discriminant analysis. In *Proceedings of the 29th International Conference on Machine Learning*, ICML’12, pages 1507–1514, USA, 2012. Omnipress. ISBN 978-1-4503-1285-1. URL <http://dl.acm.org/citation.cfm?id=3042573.3042766>.
- Kenneth L. Clarkson and David P. Woodruff. Low-rank approximation and regression in input sparsity time. *J. ACM*, 63(6):54:1–54:45, January 2017. ISSN 0004-5411. doi: 10.1145/3019134. URL <http://doi.acm.org/10.1145/3019134>.
- Paramveer Dhillon, Dean P Foster, and Lyle H Ungar. Multi-view learning of word embeddings via CCA. In *Advances in Neural Information Processing Systems*, pages 199–207, 2011.
- Paramveer S. Dhillon, Jordan Rodu, Dean P. Foster, and Lyle H. Ungar. Two step CCA: A new spectral method for estimating vector models of words. In *Proceedings of the 29th International Conference on Machine Learning*, ICML’12, pages 67–74, USA, 2012. Omnipress. ISBN 978-1-4503-1285-1. URL <http://dl.acm.org/citation.cfm?id=3042573.3042586>.
- Petros Drineas, Michael W Mahoney, S Muthukrishnan, and Tamás Sarlós. Faster least squares approximation. *Numerische Mathematik*, 117(2):219–249, 2011.
- A. Edelman, T. Arias, and S. Smith. The geometry of algorithms with orthogonality constraints. *SIAM Journal on Matrix Analysis and Applications*, 20(2):303–353, 1998. doi: 10.1137/S0895479895290954. URL <https://doi.org/10.1137/S0895479895290954>.
- Ronald A Fisher. The use of multiple measurements in taxonomic problems. *Annals of Eugenics*, 7(2):179–188, 1936.
- Jerome Friedman, Trevor Hastie, and Robert Tibshirani. *The Elements of Statistical Learning*, volume 1. Springer Series in Statistics, New York, NY, USA, 2001.

- Rong Ge, Chi Jin, Praneeth Netrapalli, Aaron Sidford, et al. Efficient algorithms for large-scale generalized eigenvector computation and canonical correlation analysis. In *International Conference on Machine Learning*, pages 2741–2750, 2016.
- Gene H Golub and Hongyuan Zha. The canonical correlations of matrix pairs and their numerical computation. In *Linear Algebra for Signal Processing*, pages 27–49. Springer, 1995.
- Alon Gonen, Francesco Orabona, and Shai Shalev-Shwartz. Solving ridge regression using sketched preconditioned SVRG. In *Proceedings of the 33rd International Conference on International Conference on Machine Learning - Volume 48*, ICML’16, pages 1397–1405. JMLR.org, 2016. URL <http://dl.acm.org/citation.cfm?id=3045390.3045538>.
- Alfred Gray, Elsa Abbena, and Simon Salamon. *Modern Differential Geometry of Curves and Surfaces with Mathematica, Third Edition (Studies in Advanced Mathematics)*. Chapman & Hall/CRC, 2006. ISBN 1584884487.
- Harold Hotelling. Relations between two sets of variates. *Biometrika*, 28(3/4):321–377, 1936.
- Tae-Kyun Kim, Josef Kittler, and Roberto Cipolla. Discriminative learning and recognition of image set classes using canonical correlations. *IEEE Transactions on Pattern Analysis and Machine Intelligence*, 29(6):1005–1018, 2007.
- Zhuang Ma, Yichao Lu, and Dean Foster. Finding linear structure in large datasets with scalable canonical correlation analysis. In *Proceedings of the 32Nd International Conference on International Conference on Machine Learning - Volume 37*, ICML’15, pages 169–178. JMLR.org, 2015. URL <http://dl.acm.org/citation.cfm?id=3045118.3045138>.
- Xiangrui Meng and Michael W. Mahoney. Low-distortion subspace embeddings in input-sparsity time and applications to robust linear regression. In *Proceedings of the Forty-fifth Annual ACM Symposium on Theory of Computing*, STOC ’13, pages 91–100, New York, NY, USA, 2013. ACM. ISBN 978-1-4503-2029-0. doi: 10.1145/2488608.2488621. URL <http://doi.acm.org/10.1145/2488608.2488621>.
- Xiangrui Meng, Michael A Saunders, and Michael W Mahoney. LSRN: A parallel iterative solver for strongly over-or underdetermined systems. *SIAM Journal on Scientific Computing*, 36(2): C95–C118, 2014.
- Sebastian Mika, Gunnar Ratsch, Jason Weston, Bernhard Scholkopf, and Klaus-Robert Mullers. Fisher discriminant analysis with kernels. In *Neural Networks for Signal Processing IX, 1999. Proceedings of the 1999 IEEE Signal Processing Society Workshop.*, pages 41–48. IEEE, 1999.
- Bamdev Mishra and Rodolphe Sepulchre. R3MC: A Riemannian three-factor algorithm for low-rank matrix completion. In *Decision and Control (CDC), 2014 IEEE 53rd Annual Conference on*, pages 1137–1142. IEEE, 2014.
- Bamdev Mishra and Rodolphe Sepulchre. Riemannian preconditioning. *SIAM Journal on Optimization*, 26(1):635–660, 2016. doi: 10.1137/140970860. URL <http://dx.doi.org/10.1137/140970860>.

- Thanh Ngo and Yousef Saad. Scaled gradients on Grassmann manifolds for matrix completion. In *Advances in Neural Information Processing Systems*, pages 1412–1420, 2012.
- Yuanming Shi, Jun Zhang, and Khaled B Letaief. Low-rank matrix completion for topological interference management by Riemannian pursuit. *arXiv preprint arXiv:1603.01729*, 2016.
- Steven T Smith. Optimization techniques on Riemannian manifolds. 1994.
- Ya Su, Yun Fu, Xinbo Gao, and Qi Tian. Discriminant learning through multiple principal angles for visual recognition. *IEEE Transactions on Image Processing*, 21(3):1381–1390, 2012.
- Liang Sun, Betul Ceran, and Jieping Ye. A scalable two-stage approach for a class of dimensionality reduction techniques. In *Proceedings of the 16th ACM SIGKDD international conference on Knowledge discovery and data mining*, pages 313–322. ACM, 2010.
- Weiran Wang, Jialei Wang, Dan Garber, and Nati Srebro. Efficient globally convergent stochastic optimization for canonical correlation analysis. In D. D. Lee, M. Sugiyama, U. V. Luxburg, I. Guyon, and R. Garnett, editors, *Advances in Neural Information Processing Systems 29*, pages 766–774. Curran Associates, Inc., 2016. URL <http://papers.nips.cc/paper/6459-efficient-globally-convergent-stochastic-opti>
- David P Woodruff et al. Sketching as a tool for numerical linear algebra. *Foundations and Trends® in Theoretical Computer Science*, 10(1–2):1–157, 2014.
- Jiyan Yang, Xiangrui Meng, and Michael W Mahoney. Implementing randomized matrix algorithms in parallel and distributed environments. *Proceedings of the IEEE*, 104(1):58–92, 2016.
- Florian Yger, Maxime Berar, Gilles Gasso, and Alain Rakotomamonjy. Adaptive canonical correlation analysis based on matrix manifolds. In *Proceedings of the 29th International Conference on International Conference on Machine Learning, ICML’12*, pages 299–306, USA, 2012. Omnipress. ISBN 978-1-4503-1285-1. URL <http://dl.acm.org/citation.cfm?id=3042573.3042615>.
- Tengfei Zhou, Hui Qian, Zebang Shen, and Congfu Xu. Riemannian tensor completion with side information. *arXiv preprint arXiv:1611.03993*, 2016.

Algorithm 1 Sketched Iterative CCA.

-
- 1: **Input:** $\mathbf{X} \in \mathbb{R}^{n \times d_x}$, $\mathbf{Y} \in \mathbb{R}^{n \times d_y}$, $s \geq \max(d_x, d_y)$, $\lambda_x, \lambda_y \geq 0$
 - 2: **Generate random** $h : \{1, \dots, d\} \rightarrow \{1, \dots, s\}$ and $g : \{1, \dots, d\} \rightarrow \{-1, +1\}$. Let \mathbf{S} denote the corresponding COUNTSKETCH matrix.
 - 3: $\mathbf{X}_S \leftarrow \mathbf{S}\mathbf{X}$, $\mathbf{Y}_S \leftarrow \mathbf{S}\mathbf{Y}$
 - 4: $\tilde{\mathbf{u}}, \tilde{\mathbf{v}} \leftarrow \text{exact-cca}(\mathbf{X}_S, \mathbf{Y}_S)$
 - 5: $\mathbf{M}_{xx} \leftarrow \mathbf{X}_S^T \mathbf{X}_S + \lambda_x \mathbf{I}_{d_x}$, $\mathbf{M}_{yy} \leftarrow \mathbf{Y}_S^T \mathbf{Y}_S + \lambda_y \mathbf{I}_{d_y}$
 - 6: **Notation:** $\Sigma_{xx} = \mathbf{X}^T \mathbf{X} + \lambda_x \mathbf{I}$, $\Sigma_{yy} = \mathbf{Y}^T \mathbf{Y} + \lambda_y \mathbf{I}$. Do not compute these matrices (algorithms only require taking products with them).
 - 7: Using Riemannian CG, solve $\max \mathbf{u}^T \mathbf{X}^T \mathbf{Y} \mathbf{v}$ s.t. $\mathbf{u} \in \mathbb{S}^{\Sigma_{xx}}$, $\mathbf{v} \in \mathbb{S}^{\Sigma_{yy}}$. Use \mathbf{M}_{xx} and \mathbf{M}_{yy} for the metric. Start the iteration from $\tilde{\mathbf{u}} / \|\tilde{\mathbf{u}}\|_{\Sigma_{xx}}$ and $\tilde{\mathbf{v}} / \|\tilde{\mathbf{v}}\|_{\Sigma_{yy}}$.
-

Algorithm 2 Sketched Iterative LDA.

-
- 1: **Input:** $\mathbf{X} \in \mathbb{R}^{n \times d}$, $\mathbf{y} \in \mathbb{N}^n$, $s \geq d$, $\lambda \geq 0$
 - 2: Compute matrices \mathbf{S}_B and $\hat{\mathbf{X}}$
 - 3: **Generate random** $h : \{1, \dots, d\} \rightarrow \{1, \dots, s\}$ and $g : \{1, \dots, d\} \rightarrow \{-1, +1\}$. Let \mathbf{S} denote the corresponding COUNTSKETCH matrix.
 - 4: $\mathbf{X}_S \leftarrow \mathbf{S}\hat{\mathbf{X}}$
 - 5: $\mathbf{M} \leftarrow \mathbf{X}_S^T \mathbf{X}_S + \lambda \mathbf{I}_d$
 - 6: Compute leading generalized eigenvector $\tilde{\mathbf{w}}$ of $(\mathbf{S}_B, \mathbf{M})$.
 - 7: **Notation:** $\mathbf{S}_w = \hat{\mathbf{X}}^T \hat{\mathbf{X}}$. Do not compute this matrix (algorithms only require taking products with it).
 - 8: Using Riemannian CG, solve $\max \mathbf{w}^T \mathbf{S}_B \mathbf{w}$ s.t. $\mathbf{w} \in \mathbb{S}^{\mathbf{S}_w + \lambda \mathbf{I}_d}$. Use \mathbf{M} for the metric. Start the iteration from $\tilde{\mathbf{w}} / \|\tilde{\mathbf{w}}\|_{\mathbf{S}_w + \lambda \mathbf{I}}$.
-

Appendix A. Related Work

Our work combines Riemannian preconditioning and sketching, and applies them to the problems of CCA and LDA (although, we believe our technique is potentially applicable to other cases of optimization with quadratic equality constraints). Here, we briefly summarize the most relevant prior work on each of these subjects.

Riemannian Preconditioning. Riemannian preconditioning was formally introduced recently by [Mishra and Sepulchre \(2016\)](#), who observed the importance of carefully selecting the metric used in Riemannian optimization. However, the practice of adjusting the metric based on the cost predates Mishra and Sepulchre’s work, see e.g. ([Ngo and Saad, 2012](#); [Mishra and Sepulchre, 2014](#); [Shi et al., 2016](#); [Zhou et al., 2016](#)). It is well-known that the condition number of the Riemannian Hessian at the optimum is highly indicative of the convergence rate of Riemannian optimization. Thus, it is desirable to select a metric that minimizes this condition number. Most of the aforementioned work attempt to do so by approximating the Euclidean Hessian of the cost function. However, it is possible for the Riemannian Hessian and the Euclidean Hessian to be very far from each other even for

simple examples (see Section 4). Indeed, our metric selection is *not* based on approximating the Euclidean Hessian. [Mishra and Sepulchre \(2016\)](#) considered the use of a metric that is both cost and constraint related. Unlike their work, when we consider concrete applications (CCA and LDA), we give simple bounds for the condition number of the Riemannian Hessian at the optimum, identify the optimal preconditioner based on the bound, and show how to efficiently approximate (using sketching) the optimal preconditioner to sufficient quality (again, measured based on the condition number of the Riemannian Hessian at the optimum).

Iterative Methods for CCA. [Golub and Zha \(1995\)](#) proposed an iterative method for CCA based on alternating least squares. Each iteration requires the solution of two least squares problems. The authors suggest using LSQR for this task. [Wang et al. \(2016\)](#) proposed to replace LSQR with either accelerated gradient descent, stochastic variance reduce gradient (SVRG) or accelerated SVRG. They also propose a different approach based on shift-and-invert preconditioning. [Ma et al. \(2015\)](#) developed an algorithm for CCA based on augmented approximate gradients. [Ge et al. \(2016\)](#) provide an iterative algorithm for the generalized eigenvalue problem, and use a standard reduction of CCA to generalized eigenvalue problems to derive an algorithm for CCA. They assume a fast black box access to an approximate linear system solver. Convergence bound of all the aforementioned algorithms depend on the condition number of the input matrices, which might be large. In contrast, the condition number bounds for our proposed sketching based algorithms are independent of the conditioning of the input matrices. Finally, we mention recent work by [Yger et al. \(2012\)](#), which uses Riemannian optimization in the context of CCA, but their setting is different from the one we consider (they consider an adaptive scenario, in which data changes over time).

Sketching. Sketching has recently emerged as a powerful technique for accelerating and scaling many important statistical learning techniques. Most of the work on sketching focused on the sketch-and-solve approach. Of particular relevance for this paper, for CCA a sketch-and-solve based approach was developed by [Avron et al. \(2014a\)](#). So far, sketch preconditioning was predominantly applied to linear least-squares regression problems (e.g., [Avron et al., 2010](#); [Meng et al., 2014](#)), and also to non-least squares variants (e.g. ℓ_1 -regression [\(Meng and Mahoney, 2013\)](#)). To the best of our knowledge, sketch preconditioning has neither been applied to CCA and LDA before, nor has it been used in the context of Riemannian optimization.

Appendix B. Riemannian Hessian on the Ellipsoid

Here we detail the derivation of the Riemannian Hessian that led to the formula stated in Section 3.

We use Definition 5.5.1 from [\(Absil et al., 2009\)](#) of the Riemannian Hessian: For a real-valued function f on \mathbb{S}^B , at a point $\mathbf{x} \in \mathbb{S}^B$ the Riemannian Hessian $\mathbf{Hess}f(\mathbf{x})$ is a linear mapping of $T_{\mathbf{x}}\mathbb{S}^B$ into itself such that $\mathbf{Hess}f(\mathbf{x})[\eta_{\mathbf{x}}] = \nabla_{\eta_{\mathbf{x}}} \text{grad}f(\mathbf{x})$, for all $\eta_{\mathbf{x}} \in T_{\mathbf{x}}\mathbb{S}^B$. In the previous equation, ∇ is the Riemannian connection, and should not be confused with the Euclidean gradient.

First, we find the Riemannian connection on \mathbb{S}^B . We can find the Riemannian connection in a similar manner to the gradient computation performed in Section 3 by using [\(Absil et al., 2009, Proposition 5.3.2\)](#), i.e. composing the connection in the ambient space with the projection on the tangent space. Let $\bar{\nabla}$ be the Levi-Civita connection on \mathbb{R}^d endowed with the metric \bar{g} . Since the metric on the ambient space \mathbb{R}^d does not depend on \mathbf{x} , $\bar{\nabla}$ is simply the classical directional derivative, and if we use the standard canonical basis $\mathbf{e}_1, \dots, \mathbf{e}_d$ to represent $\bar{\eta}_{\mathbf{x}} \in T_{\mathbf{x}}\mathbb{R}^d$ and $\bar{v} \in$

$\mathfrak{X}(\mathbb{R}^d)$ we have:

$$\bar{\nabla}_{\bar{\eta}_{\mathbf{x}}} v = \mathbf{J}_{\bar{v}(\mathbf{x})} \bar{\eta}_{\mathbf{x}}.$$

where $\mathbf{J}_{\bar{v}(\mathbf{x})}$ denotes the Jacobian matrix of \bar{v} at \mathbf{x} . Now that we have the connection on the ambient space \mathbb{R}^d , which is a Riemannian manifold, we can compute the connection on the submanifold $\mathbb{S}^{\mathbf{B}}$. Given $\eta_{\mathbf{x}} \in T_{\mathbf{x}}\mathbb{S}^{\mathbf{B}}$ and a vector field v on $\mathbb{S}^{\mathbf{B}}$, the Riemannian connection is (written, as usual, in terms of ambient coordinates)

$$\nabla_{\eta_{\mathbf{x}}} v = \mathbf{P}_{\mathbf{x}} \bar{\nabla}_{\eta_{\mathbf{x}}} \bar{v} = \mathbf{P}_{\mathbf{x}} \mathbf{J}_{\bar{v}(\mathbf{x})} \eta_{\mathbf{x}} \quad (18)$$

where $\bar{v}(\mathbf{x})$ is any smooth local extension of v in a neighborhood of $\mathbf{x} \in \mathbb{S}^{\mathbf{B}}$ in \mathbb{R}^d .

Next, we can find the Riemannian Hessian using Eq. (18), the product rule for derivation and according to (Absil et al., 2013):

$$\begin{aligned} \text{Hess} f(\mathbf{x})[\eta_{\mathbf{x}}] &= \mathbf{P}_{\mathbf{x}} \mathbf{J}_{h(\mathbf{x})} \eta_{\mathbf{x}} \\ &= \mathbf{P}_{\mathbf{x}} \mathbf{M}^{-1} \nabla^2 \bar{f}(\mathbf{x}) \eta_{\mathbf{x}} + \mathbf{P}_{\mathbf{x}} (\text{DP})(\mathbf{x})[\eta_{\mathbf{x}}] \mathbf{M}^{-1} \nabla \bar{f}(\mathbf{x}), \end{aligned} \quad (19)$$

where $\nabla \bar{f}(\mathbf{x})$ and $\nabla^2 \bar{f}(\mathbf{x})$ are the Euclidean gradient and Hessian (respectively) of \bar{f} and

$$h : \mathbb{R}^d \rightarrow \mathbb{R}^d, \quad h(\mathbf{x}) := \mathbf{P}_{\mathbf{x}} \mathbf{M}^{-1} \nabla \bar{f}(\mathbf{x}).$$

Note that for $\mathbf{x} \in \mathbb{S}^{\mathbf{B}}$ we have $h(\mathbf{x}) = \mathbf{grad} f(\mathbf{x})$ so h is a smooth local extension of the vector field $\mathbf{grad} f$ to \mathbb{R}^d , and its Jacobian is calculated as follows

$$\mathbf{J}_{h(\mathbf{x})} \eta_{\mathbf{x}} = (\text{DP})(\mathbf{x})[\eta_{\mathbf{x}}] \mathbf{M}^{-1} \nabla \bar{f}(\mathbf{x}) + \mathbf{P}_{\mathbf{x}} \mathbf{M}^{-1} \nabla^2 \bar{f}(\mathbf{x}) \eta_{\mathbf{x}},$$

where $(\text{DP})(\mathbf{x})[\eta_{\mathbf{x}}]$ (here and in Eq. (19)) is the derivative at \mathbf{x} along $\eta_{\mathbf{x}}$ of the function that maps \mathbf{x} to $\mathbf{P}_{\mathbf{x}}$. Note that once an orthonormal basis is chosen for the ambient space, $\mathbf{P}_{\mathbf{x}}$ is represented as a matrix. Hence, \mathbf{P} can be viewed as a matrix-valued function on $\mathbb{S}^{\mathbf{B}}$. Therefore, $(\text{DP})(\mathbf{x})[\eta_{\mathbf{x}}]$ (i.e., the directional derivative) is also a matrix. Moreover, the expression $(\text{DP})(\mathbf{x})[\eta_{\mathbf{x}}] \mathbf{M}^{-1} \nabla \bar{f}(\mathbf{x})$ is linear in $\eta_{\mathbf{x}}$.

The main challenge in computing the Riemannian Hessian from Eq. (19) is in computing $(\text{DP})(\mathbf{x})[\eta_{\mathbf{x}}]$. In order to circumvent this issue, we use a simple modification of a result due to Absil et al. (2013) to the case in which the Riemannian metric induced from \mathbb{R}^d on any Riemannian submanifold of \mathbb{R}^d is of the form $g_{\mathbf{x}}(\xi_{\mathbf{x}}, \eta_{\mathbf{x}}) = \xi_{\mathbf{x}}^T \mathbf{M} \eta_{\mathbf{x}}$ where $\mathbf{M} \in \mathbb{R}^{d \times d}$ is any constan, SPD matrix. In order to so, first we introduce the notion of the *Weingarten map* (also known as the *shape operator*).

Definition 11 (Weingarten map. Expansion of (Gray et al., 2006, Definition 13.1) and (Absil et al., 2013, Definition 1) from \mathbb{R}^3 to \mathbb{R}^d) Given a Riemannian manifold \mathcal{M} , a point $\mathbf{x} \in \mathcal{M}$ on the manifold, a tangent vector $\eta_{\mathbf{x}} \in T_{\mathbf{x}}\mathcal{M}$ at \mathbf{x} , and a normal vector $\mathbf{u} \in (T_{\mathbf{x}}\mathcal{M})^{\perp}$, we define the Weingarten map by

$$W_{\mathbf{x}}(\eta_{\mathbf{x}}, \mathbf{u}) := -\nabla_{\eta_{\mathbf{x}}} U. \quad (20)$$

where U is a smooth normal vector field on \mathcal{M} which is a local extension of \mathbf{u} . Naturally, the Weingarten map is linear in $\eta_{\mathbf{x}}$.

For the manifold \mathbb{S}^B , viewed as an embedded submanifold of \mathbb{R}^d , Eq. (20) reduces to $W_{\mathbf{x}}(\eta_{\mathbf{x}}, \mathbf{u}) = -\mathbf{P}_{\mathbf{x}}\mathbf{J}_{\bar{U}(\mathbf{x})}\eta_{\mathbf{x}}$ where \bar{U} is a smooth extension of U to \mathbb{R}^d . Now, recall that any normal vector \mathbf{u} on \mathbb{S}^B at \mathbf{x} is of the form $\mathbf{u} = \alpha\mathbf{M}^{-1}\mathbf{B}\mathbf{x}$ where $\alpha \in \mathbb{R}$. We can find α by left multiplying by $\mathbf{x}^T\mathbf{M}$. Indeed, after left multiplying by $\mathbf{x}^T\mathbf{M}$ we get $\mathbf{x}^T\mathbf{M}\mathbf{u} = \alpha\mathbf{x}^T\mathbf{M}\mathbf{M}^{-1}\mathbf{B}\mathbf{x} = \alpha$. Now we can define the normal field U by $U(\mathbf{x}) = \alpha\mathbf{M}^{-1}\mathbf{B}\mathbf{x}$. Obviously, it is normal field, and $U(\mathbf{x}) = \mathbf{u}$, so it is a local extension of \mathbf{u} . Next, we calculate Jacobian of $U(\mathbf{x})$:

$$\mathbf{J}_{\bar{U}(\mathbf{x})} = \alpha\mathbf{M}^{-1}\mathbf{B}.$$

Thus, the Weingarten map for \mathbb{S}^B is

$$W_{\mathbf{x}}(\eta_{\mathbf{x}}, \mathbf{u}) = -\mathbf{P}_{\mathbf{x}}(\alpha\mathbf{M}^{-1}\mathbf{B})\eta_{\mathbf{x}}. \quad (21)$$

The following Lemma is a simple modification of (Absil et al., 2013, Theorem 1). Although the proof is almost identical, we include it here for completeness.

Lemma 12 *For the Riemannian submanifold \mathbb{S}^B of \mathbb{R}^d endowed with $\bar{g}_{\mathbf{x}}(\bar{\xi}_{\mathbf{x}}, \bar{\eta}_{\mathbf{x}}) = \bar{\xi}_{\mathbf{x}}^T\mathbf{M}\bar{\eta}_{\mathbf{x}}$ we have*

$$\begin{aligned} W_{\mathbf{x}}(\eta_{\mathbf{x}}, \mathbf{P}_{\mathbf{x}}^{\perp}\mathbf{M}^{-1}\mathbf{u}) &= \mathbf{P}_{\mathbf{x}}(\mathbf{DP})(\mathbf{x})[\eta_{\mathbf{x}}]\mathbf{M}^{-1}\mathbf{u} \\ &= \mathbf{P}_{\mathbf{x}}(\mathbf{DP})(\mathbf{x})[\eta_{\mathbf{x}}]\mathbf{P}_{\mathbf{x}}^{\perp}\mathbf{M}^{-1}\mathbf{u}, \end{aligned}$$

for all $\mathbf{x} \in \mathbb{S}^B$, $\eta_{\mathbf{x}} \in T_{\mathbf{x}}\mathbb{S}^B$ and $\mathbf{u} \in \mathbb{R}^d$.

Proof First, in the proof presented in (Absil et al., 2013) they show that

$$\mathbf{P}_{\mathbf{x}}(\mathbf{DP})(\mathbf{x})[\eta_{\mathbf{x}}] = \mathbf{P}_{\mathbf{x}}(\mathbf{DP})(\mathbf{x})[\eta_{\mathbf{x}}]\mathbf{P}_{\mathbf{x}}^{\perp} \quad (22)$$

holds. Then applying both sided on $\mathbf{M}^{-1}\mathbf{u}$ gives us the equality

$$\mathbf{P}_{\mathbf{x}}(\mathbf{DP})(\mathbf{x})[\eta_{\mathbf{x}}]\mathbf{M}^{-1}\mathbf{u} = \mathbf{P}_{\mathbf{x}}(\mathbf{DP})(\mathbf{x})[\eta_{\mathbf{x}}]\mathbf{P}_{\mathbf{x}}^{\perp}\mathbf{M}^{-1}\mathbf{u}.$$

To conclude the proof we show that $W_{\mathbf{x}}(\eta_{\mathbf{x}}, \mathbf{P}_{\mathbf{x}}^{\perp}\mathbf{M}^{-1}\mathbf{u}) = \mathbf{P}_{\mathbf{x}}(\mathbf{DP})(\mathbf{x})[\eta_{\mathbf{x}}]\mathbf{M}^{-1}\mathbf{u}$. Note that for embedding submanifolds of \mathbb{R}^d with a metric derived from \mathbf{M} , the Weingarten map reduces to $W_{\mathbf{x}}(\eta_{\mathbf{x}}, \mathbf{u}) = -\mathbf{P}_{\mathbf{x}}\mathbf{J}_{\bar{U}(\mathbf{x})}\eta_{\mathbf{x}}$. Using Definition 11 along this observation, we have

$$W_{\mathbf{x}}(\eta_{\mathbf{x}}, \mathbf{P}_{\mathbf{x}}^{\perp}\mathbf{M}^{-1}\mathbf{u}) = -\mathbf{P}_{\mathbf{x}}\mathbf{J}_{\mathbf{P}_{\mathbf{x}}^{\perp}\mathbf{M}^{-1}\bar{U}(\mathbf{x})}\eta_{\mathbf{x}} \quad (23)$$

$$= -\mathbf{P}_{\mathbf{x}}(\mathbf{DP}^{\perp})(\mathbf{x})[\eta_{\mathbf{x}}]\mathbf{M}^{-1}\mathbf{u} - \mathbf{P}_{\mathbf{x}}\mathbf{P}_{\mathbf{x}}^{\perp}\mathbf{J}_{\mathbf{M}^{-1}\bar{U}(\mathbf{x})}\eta_{\mathbf{x}} \quad (24)$$

$$= \mathbf{P}_{\mathbf{x}}(\mathbf{DP})(\mathbf{x})[\eta_{\mathbf{x}}]\mathbf{M}^{-1}\mathbf{u}, \quad (25)$$

where in the last equality we used $\mathbf{P}_{\mathbf{x}}\mathbf{P}_{\mathbf{x}}^{\perp} = 0$ and $\mathbf{P}^{\perp} = \mathbf{I} - \mathbf{P}$. ■

As a consequence of Lemma 12, we can replace $\mathbf{P}_{\mathbf{x}}(\mathbf{DP})(\mathbf{x})[\eta_{\mathbf{x}}]\mathbf{M}^{-1}\nabla\bar{f}(\mathbf{x})$ by $W_{\mathbf{x}}(\eta_{\mathbf{x}}, \mathbf{P}_{\mathbf{x}}^{\perp}\mathbf{M}^{-1}\nabla\bar{f}(\mathbf{x}))$ in Eq. (19). Therefore the expression for the Riemannian Hessian becomes

$$\text{Hess}f(\mathbf{x})[\eta_{\mathbf{x}}] = \mathbf{P}_{\mathbf{x}}\mathbf{M}^{-1}\nabla^2\bar{f}(\mathbf{x})\eta_{\mathbf{x}} + W_{\mathbf{x}}(\eta_{\mathbf{x}}, \mathbf{P}_{\mathbf{x}}^{\perp}\mathbf{M}^{-1}\nabla\bar{f}(\mathbf{x})). \quad (26)$$

In particular, the Riemannian Hessian on $\mathbb{S}^{\mathbf{B}}$ is

$$\begin{aligned} \text{Hess}f(\mathbf{x})[\eta_{\mathbf{x}}] &= \mathbf{P}_{\mathbf{x}}\mathbf{M}^{-1}\nabla^2\bar{f}(\mathbf{x})\eta_{\mathbf{x}} - \mathbf{P}_{\mathbf{x}}((\mathbf{x}^T\mathbf{M}\mathbf{P}_{\mathbf{x}}^{\perp}\mathbf{M}^{-1}\nabla\bar{f}(\mathbf{x}))\mathbf{M}^{-1}\mathbf{B})\eta_{\mathbf{x}} \\ &= \mathbf{P}_{\mathbf{x}}\mathbf{M}^{-1}[\nabla^2\bar{f}(\mathbf{x}) - (\mathbf{x}^T\nabla\bar{f}(\mathbf{x}) - \mathbf{x}^T\mathbf{M}\mathbf{P}_{\mathbf{x}}\mathbf{M}^{-1}\nabla\bar{f}(\mathbf{x}))\mathbf{B}]\eta_{\mathbf{x}} \\ &= \mathbf{P}_{\mathbf{x}}\mathbf{M}^{-1}[\nabla^2\bar{f}(\mathbf{x}) - (\mathbf{x}^T\nabla\bar{f}(\mathbf{x}) - g_{\mathbf{x}}(\mathbf{x}, \text{grad}f(\mathbf{x}))\mathbf{B})\eta_{\mathbf{x}}]. \end{aligned}$$

In the case $\mathbf{M} = \mathbf{B}$ the formula simplifies to

$$\text{Hess}f(\mathbf{x})[\eta_{\mathbf{x}}] = \mathbf{P}_{\mathbf{x}}\mathbf{B}^{-1}[\nabla^2\bar{f}(\mathbf{x}) - \mathbf{x}^T\nabla\bar{f}(\mathbf{x})\mathbf{B}]\eta_{\mathbf{x}}.$$

Appendix C. Product Manifold of Ellipsoids

In some cases, it is desirable to solve optimization problems with several variables, in which each is constrained to a different ellipsoid. For example, in Section 5 the CCA problem is formulated as an optimization problem with two quadratic equality constraints. Such cases are easily addressed by using the notion of *product manifold* (see also Section 3.1.6 in Absil et al. (2009)). Here, we briefly summarize how it applies to our settings.

Let $\mathbf{B}_1, \dots, \mathbf{B}_k$ be SPD matrices, where the dimension of \mathbf{B}_i is $d_i \times d_i$, and denote $d = d_1 + \dots + d_k$. Suppose we wish to minimize $f(\mathbf{x}_1, \dots, \mathbf{x}_k)$ where we constraint $\mathbf{x}_i \in \mathbb{S}^{\mathbf{B}_i}$ for $i = 1, \dots, k$. We can solve this problem using Riemannian optimization on the product manifold $\mathbb{S}^{\mathbf{B}_1} \times \mathbb{S}^{\mathbf{B}_2} \times \dots \times \mathbb{S}^{\mathbf{B}_k}$. Indeed, for the product manifold, there is a natural way to define the differentiable structure so that manifold topology of $\mathbb{S}^{\mathbf{B}_1} \times \mathbb{S}^{\mathbf{B}_2} \times \dots \times \mathbb{S}^{\mathbf{B}_k}$ is the product topology. However, to employ Riemannian optimization we also need to define a metric on the product manifold.

Suppose that on each $\mathbb{S}^{\mathbf{B}_i}$ we use the metric defined by a SPD matrix \mathbf{M}_i (i.e., the metric $g^{(i)}$ on $\mathbb{S}^{\mathbf{B}_i}$ is defined in ambient coordinates by $g_{\mathbf{x}}^{(i)}(\eta_{\mathbf{x}}, \xi_{\mathbf{x}}) = \eta_{\mathbf{x}}^T \mathbf{M}_i \xi_{\mathbf{x}}$). The product manifold $\mathbb{S}^{\mathbf{B}_1} \times \mathbb{S}^{\mathbf{B}_2} \times \dots \times \mathbb{S}^{\mathbf{B}_k}$ is a Riemannian submanifold of $\mathbb{R}^{d_1} \times \mathbb{R}^{d_2} \times \dots \times \mathbb{R}^{d_k}$ endowed with the product metric (sum of the metric values on each product component). Since $\mathbb{R}^{d_1} \times \mathbb{R}^{d_2} \times \dots \times \mathbb{R}^{d_k}$ is naturally isomorphic to \mathbb{R}^d by stacking the different components, then we can view $\mathbb{S}^{\mathbf{B}_1} \times \mathbb{S}^{\mathbf{B}_2} \times \dots \times \mathbb{S}^{\mathbf{B}_k}$ as a Riemannian embedded submanifold of \mathbb{R}^d endowed by the metric defined by the $d \times d$ matrix

$$\mathbf{M} = \begin{bmatrix} \mathbf{M}_1 & & & \\ & \mathbf{M}_2 & & \\ & & \ddots & \\ & & & \mathbf{M}_k \end{bmatrix}$$

The various notions introduced in previous subsections now extend to the product manifold in a straight forward way. Indeed, the tangent space of $\mathbb{S}^{\mathbf{B}_1} \times \dots \times \mathbb{S}^{\mathbf{B}_k}$ is the product of tangent spaces of each of the ellipsoids. The retraction and vector transport is the column-stack of the retractions and vector transports on each of the ellipsoids. The Riemannian gradient is computed using the orthogonal projection to the tangent space after premultiplying by \mathbf{M}^{-1} , i.e. $\text{grad}f(\mathbf{x}) = \mathbf{P}_{\mathbf{x}}\mathbf{M}^{-1}\nabla\bar{f}(\mathbf{x})$ for $\mathbf{x} \in \mathbb{S}^{\mathbf{B}_1} \times \dots \times \mathbb{S}^{\mathbf{B}_k}$, where $\mathbf{P}_{\mathbf{x}} = \text{diag}(\mathbf{P}_{\mathbf{x}_1}, \dots, \mathbf{P}_{\mathbf{x}_k})$, and $\mathbf{P}_{\mathbf{x}_i}$ is the orthogonal projection to $T_{\mathbf{x}_i}\mathbb{S}^{\mathbf{B}_i}$. The normal space is the product of the normal spaces of the ellipsoid, and therefore the Weingarten map is of the form

$$W_{\mathbf{x}}(\eta_{\mathbf{x}}, \mathbf{u}) = -\mathbf{P}_{\mathbf{x}}(\text{diag}(\alpha_1 \cdot \mathbf{I}_{d_1}, \dots, \alpha_k \cdot \mathbf{I}_{d_k})\mathbf{M}^{-1}\mathbf{B})\eta_{\mathbf{x}}, \quad (27)$$

where $\mathbf{B} = \text{diag}(\mathbf{B}_1, \dots, \mathbf{B}_k)$, $\mathbf{u} \in (T_{\mathbf{x}}\mathbb{S}^{\mathbf{B}_1} \times \dots \times \mathbb{S}^{\mathbf{B}_k})^\perp$ is a column stack of normal components and $\alpha_i = \mathbf{x}_i^\top \mathbf{M}_i \mathbf{u}_i$. Note that $\text{diag}(\alpha_1 \cdot \mathbf{I}_{d_1}, \dots, \alpha_k \cdot \mathbf{I}_{d_k})$ and \mathbf{M}^{-1} commute. The Riemannian Hessian can be computed using Eq. (26) since Lemma 12 holds for the product manifold as well.

Appendix D. Numerical Experiments

We report preliminary experiments with our proposed CCA and LDA algorithms. Our experiments are not designed to be exhaustive; we use a prototype MATLAB implementation. Our goal is to exemplify the use of preconditioning in the context of CCA and LDA. In particular, we aim to show that these problems can be solved using Riemannian optimization, that the optimization algorithm can be preconditioned, that the convergence depends on how well the preconditioner approximates the best preconditioner, and finally that sketching provides an effective way to form the preconditioner.

We experiment with two different preconditioning strategies. The first is the preconditioning strategy describe in Section 6, which we term in the graphs as “Subspace Embedding Preconditioning”. The second is the preconditioning strategy described by Gonen et al. (2016), which we term as “Dominant Subspace Preconditioning”. Suppose $\mathbf{A} \in \mathbb{R}^{d \times d}$ be some SPD matrix, and let $\mathbf{A} = \mathbf{U}\mathbf{\Lambda}\mathbf{U}^\top$ be an eigendecomposition, with the diagonal entries in $\mathbf{\Lambda}$ sorted in descending order. Given k , let us denote by \mathbf{U}_k the first k columns of \mathbf{U} , $\mathbf{\Lambda}_k$ denote the leading $k \times k$ minor of $\mathbf{\Lambda}$, and λ_k the k largest eigenvalue of \mathbf{A} . The k -dominant subspace preconditioner of $\mathbf{A} + \lambda \mathbf{I}_d$ is $\mathbf{U}(\mathbf{\Lambda} - \lambda_k \mathbf{I})\mathbf{U}^\top + (\lambda_k + \lambda)\mathbf{I}_d$. The dominant subspace can be found using a sparse SVD solver (we use MATLAB’s `svds`). We use this method to precondition $\Sigma_{\mathbf{x}\mathbf{x}}$ and $\Sigma_{\mathbf{y}\mathbf{y}}$ for CCA, and $\mathbf{S}_{\mathbf{w}} + \lambda \mathbf{I}_d$ for LDA.

We use MATLAB for our implementations, relying on the MANOPT library for Riemannian optimization. We tested the use of both Riemannian CG and Riemannian Trust Region Method. We did not optimize the implementation, so as a performance metric we use passes over the input data (which is the dominant cost in our algorithms). For CG, this directly corresponds to number of iterations, since each iteration does a fixed amount of passes over the data, so we simply report this metric. For the Trust Region Method, different iterations do a variable amount of passes, so we measure passes directly. Against the iteration/passes count we plot the suboptimality of the current iterate: $|\sigma_1 - \mathbf{u}_k^\top \Sigma_{\mathbf{x}\mathbf{y}} \mathbf{v}_k| / \sigma_1$ for CCA and $|\rho_1 - \mathbf{w}_k^\top \mathbf{S}_{\mathbf{B}} \mathbf{w}_k| / \rho_1$ for LDA.

We use three datasets: MNIST, MEDIAMILL and COVTYPE⁵. MNIST is used for testing CCA and LDA, where for CCA we try to correlate the left side of the image to the right side of the image. MEDIAMILL is a multilabel dataset, so we use it to test CCA. COVTYPE is a large (581,012 examples) labeled dataset, and we use it to test LDA.

Results for MNIST appear in Figure 1 (for CCA) and Figure 2 (for LDA). Consider Figure 1 (CCA). As a reference, for CCA the number of iterations required for CG with the best preconditioner ($\mathbf{M} = \Sigma$) is 47 and the number of iterations required for the worst preconditioner (identity) is 200. We clearly see the direct correspondence between sketch quality (as measured by sketch size) and number of passes over the data. Furthermore, the number of iterations is close to optimal after sketching to only 2000 examples (there are 60,000 examples in the original dataset) or using only 40 singular vectors (there are 784 features in the dataset)⁶. Next, consider Figure 2 (LDA).

5. Datasets were downloaded for LIBSVM’s website: <https://www.csie.ntu.edu.tw/~cjlin/libsvmtools/datasets/>

6. Interestingly, with $s \geq 500$ the subspace embedding preconditioner uses less iterations than the optimal preconditioner. This is because of the use of sketching based warm-start.

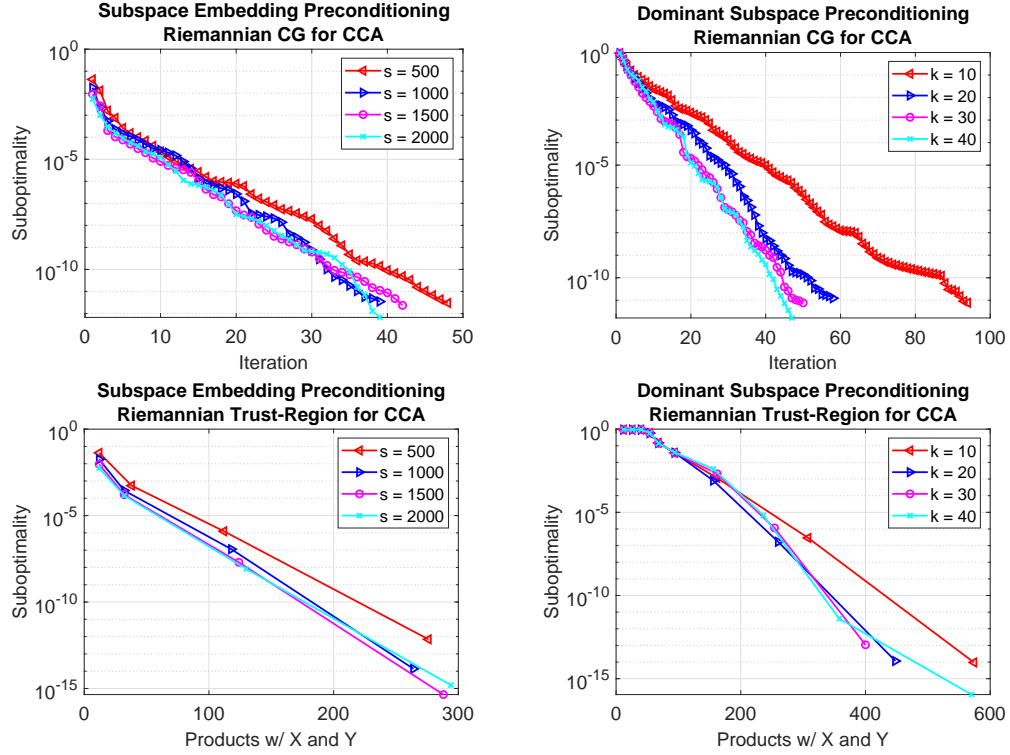


Figure 1: Results for CCA on MNIST.

As a reference, for LDA the number of iterations required for CG with the best preconditioner ($\mathbf{M} = \mathbf{S}_w + \lambda \mathbf{I}_d$) is 35 and the number of iterations required for the worst preconditioner (identity) is 833, so again we see that the sketching is effective for this problem.

Results for MEDIAMILL appear in Figure 3 (results are for CCA). As a reference, the number of iterations required for CG with the best preconditioner ($\mathbf{M} = \Sigma$) is 17 and the number of iterations required for the worst preconditioner (identity) is 72. The dataset has 30,993 examples and 221 features, so again we see that we can sketch to relatively small size ($s = 2000$ or $k = 40$) and get an effective preconditioner.

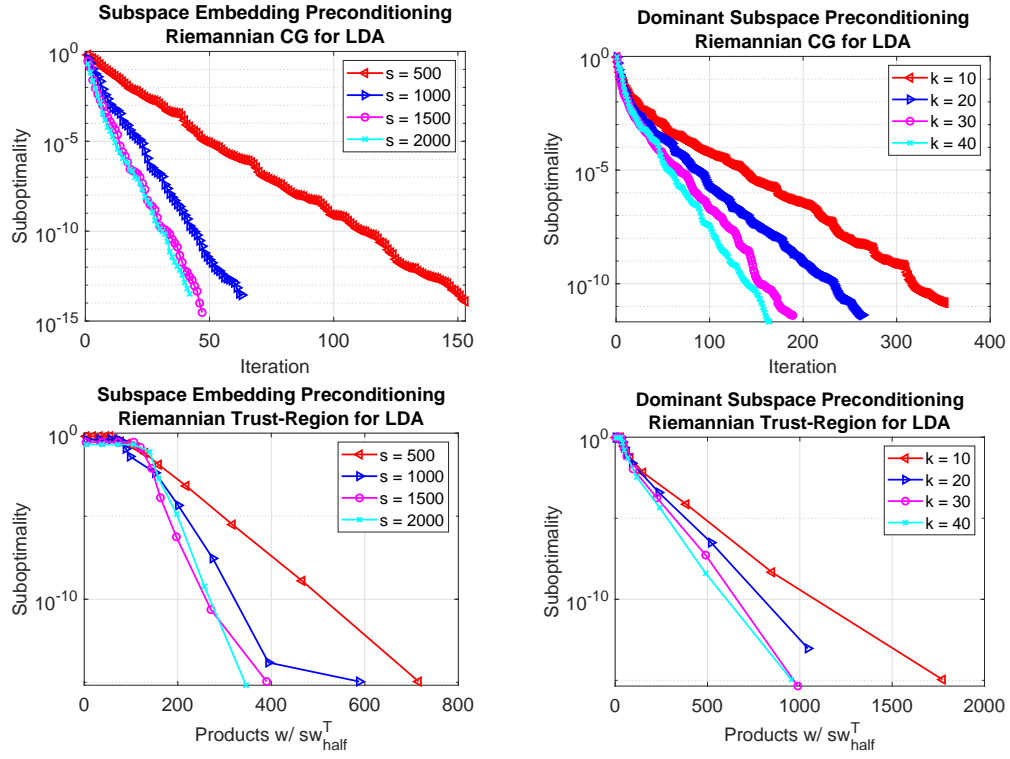


Figure 2: Results for LDA on MNIST.

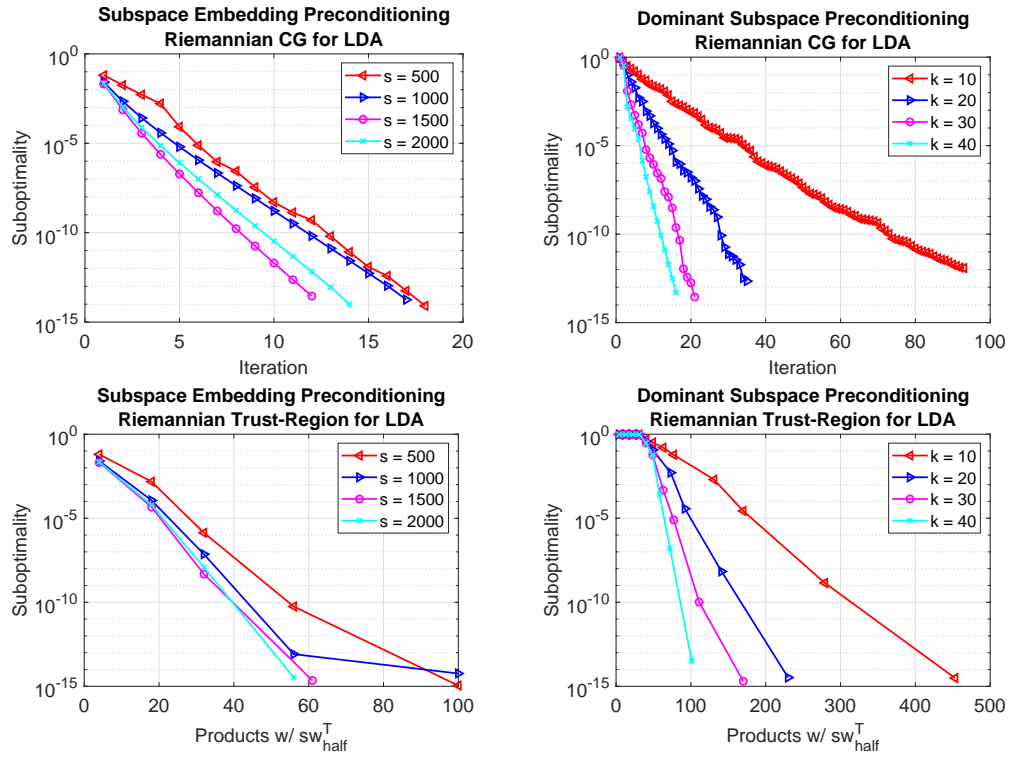


Figure 4: Results for LDA on COVTYPE.

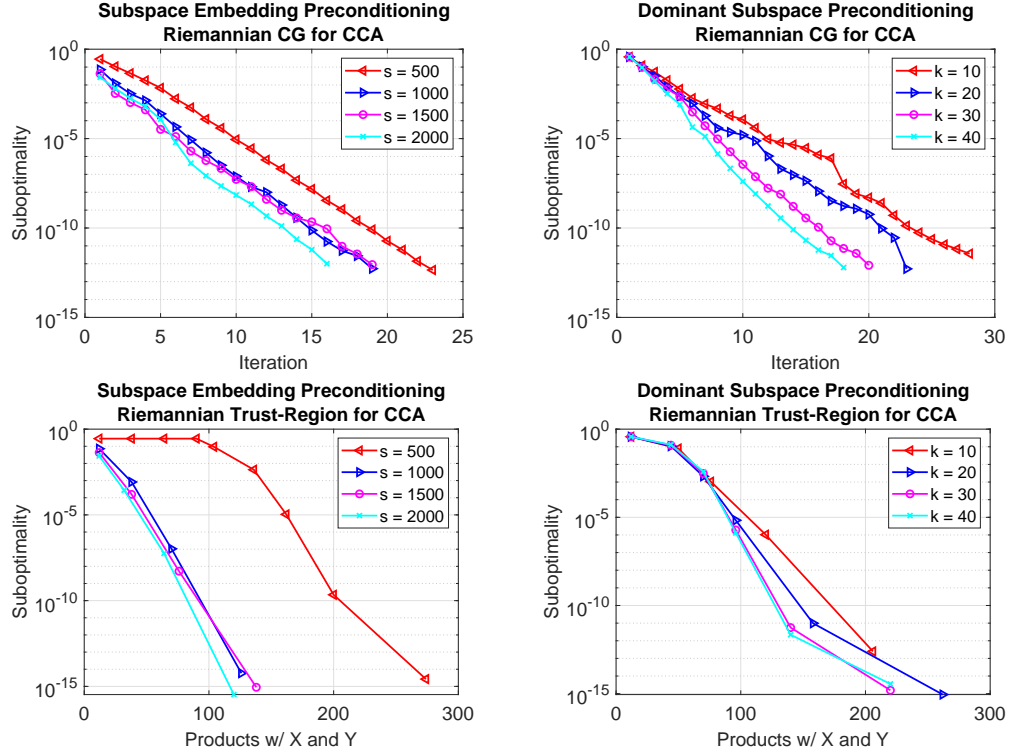


Figure 3: Results for CCA on MEDIAMILL.

Results for COVTYPE appear in Figure 4 (results are for LDA). As a reference, the number of iterations required for CG with the best preconditioner ($\mathbf{M} = \Sigma$) is 292 and the number of iterations required for the worst preconditioner (identity) is 72. Considering that the dataset has over half a million examples, subspace embedding preconditioning is highly effective, as it sketches the data to a comparatively very small size. The dataset has only 50 features, so dominant subspace preconditioning is less effective for this dataset.

Appendix E. Omitted Proofs

E.1. Proof of Lemma 1

Tangent Space. The tangent space at $\mathbf{x} \in \mathbb{S}^{\mathbf{B}}$, $T_{\mathbf{x}}\mathbb{S}^{\mathbf{B}}$, viewed as a subspace of $T_{\mathbf{x}}\mathbb{R}^d \simeq \mathbb{R}^d$, is

$$T_{\mathbf{x}}\mathbb{S}^{\mathbf{B}} = \left\{ \mathbf{z} \in \mathbb{R}^d : \mathbf{z}^T \mathbf{B} \mathbf{x} = 0 \right\}.$$

To see this, note that $\mathbb{S}^{\mathbf{B}}$ is the level set of $F(\mathbf{x}) = \mathbf{x}^T \mathbf{B} \mathbf{x} - 1$, so $T_{\mathbf{x}}\mathbb{S}^{\mathbf{B}} = \ker(DF(\mathbf{x}))$, with $DF(\mathbf{x})[\mathbf{z}] = 2\mathbf{z}^T \mathbf{B} \mathbf{x}$. In the previous line, $DF(\mathbf{x})$ denotes the *differential* of F at \mathbf{x} , i.e. the linear mapping that maps a direction \mathbf{v} to the derivative of F in direction \mathbf{v} at \mathbf{x} .

Retraction. To derive a retraction on $\mathbb{S}^{\mathbf{B}}$, we use (Absil et al., 2009, Proposition 4.1.2). Define the diffeomorphism

$$\phi : \mathbb{S}^{\mathbf{B}} \times (0, \infty) \rightarrow (\mathbb{R}^d - \{0\}), \quad \phi(\mathbf{x}, r) := \mathbf{x}r$$

Obviously, $\phi^{-1}(\mathbf{z}) = (\mathbf{z}/\|\mathbf{z}\|_{\mathbf{B}}, \|\mathbf{z}\|_{\mathbf{B}})$, so according to the aforementioned proposition

$$R_{\mathbf{x}}(\xi) := \pi_1(\phi^{-1}(\mathbf{x} + \xi)) = \frac{\mathbf{x} + \xi}{\|\mathbf{x} + \xi\|_{\mathbf{B}}}$$

defines a retraction for $\mathbb{S}^{\mathbf{B}}$, where $\mathbf{x} \in \mathbb{S}^{\mathbf{B}}$ and $\xi \in T_{\mathbf{x}}\mathbb{S}^{\mathbf{B}}$. In the above, π_1 is the projection on the first component of the pair, i.e $\pi_1(\mathbf{x}, r) = \mathbf{x}$.

Vector Transport. A vector transport can be derived by differentiating the retraction defined by Eq. (4) (Absil et al., 2009, Section 8.1.2):

$$\begin{aligned} \mathcal{T}_{\eta_{\mathbf{x}}}(\xi_{\mathbf{x}}) &:= \mathbf{D}R_{\mathbf{x}}(\eta_{\mathbf{x}})[\xi_{\mathbf{x}}] = \left. \frac{d}{dt} R_{\mathbf{x}}(\eta_{\mathbf{x}} + t\xi_{\mathbf{x}}) \right|_{t=0} \\ &= \frac{1}{\|\mathbf{x} + \eta_{\mathbf{x}}\|_{\mathbf{B}}} \left[\mathbf{I} - \frac{(\mathbf{x} + \eta_{\mathbf{x}})(\mathbf{x} + \eta_{\mathbf{x}})^{\mathbf{T}} \mathbf{B}}{\|\mathbf{x} + \eta_{\mathbf{x}}\|_{\mathbf{B}}^2} \right] \xi_{\mathbf{x}}. \end{aligned}$$

E.2. Proof of Lemma 3

First, we recall that if a projection matrix \mathbf{P} defines an orthogonal projection with respect to $(\cdot, \cdot)_{\mathbf{M}}$ then it must be self-adjoint with respect to that inner product, that is $(\mathbf{P}\mathbf{x}, \mathbf{y})_{\mathbf{M}} = (\mathbf{x}, \mathbf{P}\mathbf{y})_{\mathbf{M}}$ for all $\mathbf{x}, \mathbf{y} \in \mathbb{R}^d$. This leads to $\mathbf{P}^{\mathbf{T}} = \mathbf{M}\mathbf{P}\mathbf{M}^{-1}$. \mathbf{P} must also be a projection matrix, so $\mathbf{P}^2 = \mathbf{P}$. Let now $\mathbf{z} \in \mathbb{R}^d$ be an arbitrary vector, and let us figure out the orthogonal projection matrix with respect to $(\cdot, \cdot)_{\mathbf{M}}$ on the span of \mathbf{z} . From the previous two observations, it is not hard to see that it is $\mathbf{P}^{(\mathbf{z})} := (\mathbf{z}^{\mathbf{T}}\mathbf{M}\mathbf{z})^{-1}\mathbf{z}\mathbf{z}^{\mathbf{T}}\mathbf{M}$. Now, since the normal space is a one-dimensional space, we can write $(T_{\mathbf{x}}\mathbb{S}^{\mathbf{B}})^{\perp} = \{\alpha\mathbf{y} : \alpha \in \mathbb{R}\}$ for some \mathbf{y} , and so $\mathbf{P}^{(\mathbf{y})}$ is the orthogonal projection with respect to $(\cdot, \cdot)_{\mathbf{M}}$ on $(T_{\mathbf{x}}\mathbb{S}^{\mathbf{B}})^{\perp}$. We then have $\mathbf{P}_{\mathbf{x}} := \mathbf{I} - \mathbf{P}^{(\mathbf{y})}$ as the desired projection on $T_{\mathbf{x}}\mathbb{S}^{\mathbf{B}}$. It remains to find an analytic expression for \mathbf{y} . Recall that for every $\xi_{\mathbf{x}} \in T_{\mathbf{x}}\mathbb{S}^{\mathbf{B}}$ we have $\xi_{\mathbf{x}}^{\mathbf{T}}\mathbf{B}\mathbf{x} = 0$, so $\xi_{\mathbf{x}}^{\mathbf{T}}\mathbf{M}(\mathbf{M}^{-1}\mathbf{B}\mathbf{x}) = 0$ and $\mathbf{y} = (\mathbf{M}^{-1}\mathbf{B}\mathbf{x})$. Thus, the orthogonal projection matrix on $(T_{\mathbf{x}}\mathbb{S}^{\mathbf{B}})^{\perp}$ is

$$\mathbf{P}_{\mathbf{x}}^{\perp} := \mathbf{P}^{(\mathbf{M}^{-1}\mathbf{B}\mathbf{x})} = (\mathbf{x}^{\mathbf{T}}\mathbf{B}\mathbf{M}^{-1}\mathbf{B}\mathbf{x})^{-1}\mathbf{M}^{-1}\mathbf{B}\mathbf{x}\mathbf{x}^{\mathbf{T}}\mathbf{B}.$$

Consequently, the projection matrix on the tangent space is

$$\mathbf{P}_{\mathbf{x}} := (\mathbf{I}_n - (\mathbf{x}^{\mathbf{T}}\mathbf{B}\mathbf{M}^{-1}\mathbf{B}\mathbf{x})^{-1}\mathbf{M}^{-1}\mathbf{B}\mathbf{x}\mathbf{x}^{\mathbf{T}}\mathbf{B}).$$

E.3. Proof of Theorem 5

The costs are evident from the various formulas once we observe that none of the operations require forming $\Sigma_{\mathbf{xx}}$, $\Sigma_{\mathbf{yy}}$ or $\Sigma_{\mathbf{xy}}$, but instead require taking product of these matrices with vectors. These products can be computed in cost proportional to the number of non-zeros in \mathbf{X} and/or \mathbf{Y} by iterated products. For example, computing $\Sigma_{\mathbf{xy}}\mathbf{w}$ can be done by first computing $\mathbf{Y}\mathbf{w}$ and then multiplying \mathbf{X} by this vector (so the cost is $O(\mathbf{nnz}(\mathbf{X}) + \mathbf{nnz}(\mathbf{Y}))$). Recall, that that projections require normalization, but this again can be computed using iterated products.

The rest of the proof is devoted to proving the condition number bound. At the optimum, $\mathbf{z}^{\star} = \begin{bmatrix} \mathbf{u}_1 \\ \mathbf{v}_1 \end{bmatrix} \in \mathbb{R}^d$ we have $f(\mathbf{z}^{\star}) = -\mathbf{u}_1^{\mathbf{T}}\Sigma_{\mathbf{xy}}\mathbf{v}_1 = -\mathbf{v}_1^{\mathbf{T}}\Sigma_{\mathbf{xy}}^{\mathbf{T}}\mathbf{u}_1 = -\sigma_1$. The formula for the Riemannian Hessian is

$$\mathbf{Hess}f(\mathbf{z})[\eta_{\mathbf{z}}] = \mathbf{P}_{\mathbf{z}}\mathbf{M}^{-1}\nabla^2\bar{f}(\mathbf{z})\eta_{\mathbf{z}} + W_{\mathbf{z}}(\eta_{\mathbf{z}}, \mathbf{P}_{\mathbf{z}}^{\perp}\mathbf{M}^{-1}\nabla\bar{f}(\mathbf{z}))$$

Noticing that for any $\mathbf{z} \in \mathbb{R}^d$, $\mathbf{P}_{\mathbf{z}}^\perp \mathbf{M}^{-1} \nabla \bar{f}(\mathbf{z}) = \mathbf{M}^{-1} \nabla \bar{f}(\mathbf{z}) - \mathbf{grad} f(\mathbf{z})$, and that at \mathbf{z}^* the Riemannian gradient $\mathbf{grad} f(\mathbf{z}^*)$ vanishes (since it is a critical point), $\mathbf{Hess} f(\mathbf{z}^*)[\eta_{\mathbf{z}}]$ is reduced to $\mathbf{P}_{\mathbf{z}^*} \mathbf{M}^{-1} \nabla^2 \bar{f}(\mathbf{z}^*) \eta_{\mathbf{z}^*} + W_{\mathbf{z}}(\eta_{\mathbf{z}^*}, \mathbf{M}^{-1} \nabla \bar{f}(\mathbf{z}^*))$. Plugging (27) we get

$$\begin{aligned} \mathbf{Hess} f(\mathbf{z}^*)[\eta_{\mathbf{z}^*}] &= \mathbf{P}_{\mathbf{z}^*} \mathbf{M}^{-1} \nabla^2 \bar{f}(\mathbf{z}^*) \eta_{\mathbf{z}^*} + W_{\mathbf{z}}(\eta_{\mathbf{z}^*}, \mathbf{M}^{-1} \nabla \bar{f}(\mathbf{z}^*)) \\ &= \mathbf{P}_{\mathbf{z}^*} \mathbf{M}^{-1} \left(\nabla^2 \bar{f}(\mathbf{z}^*) + \begin{bmatrix} (\mathbf{u}_1^\top \Sigma_{\mathbf{x}\mathbf{y}} \mathbf{v}_1) \cdot \Sigma_{\mathbf{x}\mathbf{x}} & 0_{d_{\mathbf{x}} \times d_{\mathbf{y}}} \\ 0_{d_{\mathbf{y}} \times d_{\mathbf{x}}} & (\mathbf{v}_1^\top \Sigma_{\mathbf{x}\mathbf{y}}^\top \mathbf{u}_1) \cdot \Sigma_{\mathbf{y}\mathbf{y}} \end{bmatrix} \right) \eta_{\mathbf{z}^*} \\ &= \mathbf{P}_{\mathbf{z}^*} \mathbf{M}^{-1} (\nabla^2 \bar{f}(\mathbf{z}^*) + \sigma_1 \cdot \Sigma) \eta_{\mathbf{z}^*} \\ &= \mathbf{P}_{\mathbf{z}^*} \mathbf{M}^{-1} \begin{bmatrix} \sigma_1 \cdot \Sigma_{\mathbf{x}\mathbf{x}} & -\Sigma_{\mathbf{x}\mathbf{y}} \\ -\Sigma_{\mathbf{y}\mathbf{x}}^\top & \sigma_1 \cdot \Sigma_{\mathbf{y}\mathbf{y}} \end{bmatrix} \eta_{\mathbf{z}^*} \end{aligned}$$

The Riemannian Hessian is self-adjoint with respect to the Riemannian metric (see Absil et al. (2009), Proposition 5.5.3), so for every $\mathbf{z} \in \mathbb{S}_{\mathbf{x}\mathbf{y}}$ we have $g_{\mathbf{x}}(\mathbf{Hess} f(\mathbf{z})[\eta_{\mathbf{z}}], \xi_{\mathbf{z}}) = g_{\mathbf{x}}(\eta_{\mathbf{z}}, \mathbf{Hess} f(\mathbf{z})[\xi_{\mathbf{z}}])$ for any $\eta_{\mathbf{z}}, \xi_{\mathbf{z}} \in T_{\mathbf{z}} \mathbb{S}_{\mathbf{x}\mathbf{y}}$. So, due to the Courant-Fisher Theorem we have

$$\begin{aligned} \lambda_{\max}(\mathbf{Hess} f(\mathbf{z}^*)) &= \max_{0 \neq \eta_{\mathbf{z}^*} \in T_{\mathbf{z}^*} \mathbb{S}_{\mathbf{x}\mathbf{y}}} \frac{g_{\mathbf{z}^*}(\eta_{\mathbf{z}^*}, \mathbf{Hess} f(\mathbf{z}^*)[\eta_{\mathbf{z}^*}])}{g_{\mathbf{z}^*}(\eta_{\mathbf{z}^*}, \eta_{\mathbf{z}^*})} \\ \lambda_{\min}(\mathbf{Hess} f(\mathbf{z}^*)) &= \min_{0 \neq \eta_{\mathbf{z}^*} \in T_{\mathbf{z}^*} \mathbb{S}_{\mathbf{x}\mathbf{y}}} \frac{g_{\mathbf{z}^*}(\eta_{\mathbf{z}^*}, \mathbf{Hess} f(\mathbf{z}^*)[\eta_{\mathbf{z}^*}])}{g_{\mathbf{z}^*}(\eta_{\mathbf{z}^*}, \eta_{\mathbf{z}^*})} \end{aligned}$$

The above is stated in a coordinate-free manner. In ambient coordinates, viewing $T_{\mathbf{z}^*} \mathbb{S}_{\mathbf{x}\mathbf{y}}$ as a subspace of \mathbb{R}^d (see Eq. (3)):

$$\begin{aligned} \lambda_{\max}(\mathbf{Hess} f(\mathbf{z}^*)) &= \max_{0 \neq \eta_{\mathbf{z}^*} \in T_{\mathbf{z}^*} \mathbb{S}_{\mathbf{x}\mathbf{y}}} \frac{(\eta_{\mathbf{z}^*}, \mathbf{Hess} f(\mathbf{z}^*)[\eta_{\mathbf{z}^*}])_{\mathbf{M}}}{(\eta_{\mathbf{z}^*}, \eta_{\mathbf{z}^*})_{\mathbf{M}}} \\ \lambda_{\min}(\mathbf{Hess} f(\mathbf{z}^*)) &= \min_{0 \neq \eta_{\mathbf{z}^*} \in T_{\mathbf{z}^*} \mathbb{S}_{\mathbf{x}\mathbf{y}}} \frac{(\eta_{\mathbf{z}^*}, \mathbf{Hess} f(\mathbf{z}^*)[\eta_{\mathbf{z}^*}])_{\mathbf{M}}}{(\eta_{\mathbf{z}^*}, \eta_{\mathbf{z}^*})_{\mathbf{M}}} \end{aligned}$$

Plugging in the ambient coordinates formula for the Hessian, the quotient in the above reduces to

$$\frac{\eta_{\mathbf{z}^*}^\top \mathbf{M} \mathbf{P}_{\mathbf{z}^*} \mathbf{M}^{-1} (\nabla^2 \bar{f}(\mathbf{z}^*) + \sigma_1 \cdot \Sigma) \eta_{\mathbf{z}^*}}{\eta_{\mathbf{z}^*}^\top \mathbf{M} \eta_{\mathbf{z}^*}}.$$

Now using $\mathbf{M} \mathbf{P}_{\mathbf{z}^*} \mathbf{M}^{-1} = \mathbf{P}_{\mathbf{z}^*}^\top$ and the fact that $\mathbf{P}_{\mathbf{z}^*}$ is a projection on $T_{\mathbf{z}^*} \mathbb{S}_{\mathbf{x}\mathbf{y}}$ so $\mathbf{P}_{\mathbf{z}^*} \eta_{\mathbf{z}^*} = \eta_{\mathbf{z}^*}$ (since $\eta_{\mathbf{z}^*} \in T_{\mathbf{z}^*} \mathbb{S}_{\mathbf{x}\mathbf{y}}$), we further see that

$$\begin{aligned} \frac{\eta_{\mathbf{z}^*}^\top \mathbf{M} \mathbf{P}_{\mathbf{z}^*} \mathbf{M}^{-1} (\nabla^2 \bar{f}(\mathbf{z}^*) + \sigma_1 \cdot \Sigma) \eta_{\mathbf{z}^*}}{\eta_{\mathbf{z}^*}^\top \mathbf{M} \eta_{\mathbf{z}^*}} &= \\ \frac{\eta_{\mathbf{z}^*}^\top (\nabla^2 \bar{f}(\mathbf{z}^*) + \sigma_1 \cdot \Sigma) \eta_{\mathbf{z}^*}}{\eta_{\mathbf{z}^*}^\top \mathbf{M} \eta_{\mathbf{z}^*}} &= \frac{\eta_{\mathbf{z}^*}^\top (\nabla^2 \bar{f}(\mathbf{z}^*) + \sigma_1 \cdot \Sigma) \eta_{\mathbf{z}^*}}{\eta_{\mathbf{z}^*}^\top \Sigma \eta_{\mathbf{z}^*}} \cdot \frac{\eta_{\mathbf{z}^*}^\top \Sigma \eta_{\mathbf{z}^*}}{\eta_{\mathbf{z}^*}^\top \mathbf{M} \eta_{\mathbf{z}^*}}. \end{aligned}$$

(where we use the fact that Σ is not singular).

Now,

$$\begin{aligned}
\lambda_{\min}(\text{Hess}f(\mathbf{z}^*)) &\geq \min_{0 \neq \eta_{\mathbf{z}^*} \in T_{\mathbf{z}^*} \mathbb{S}_{\mathbf{xy}}} \frac{\eta_{\mathbf{z}^*}^T (\nabla^2 \bar{f}(\mathbf{z}^*) + \sigma_1 \cdot \Sigma) \eta_{\mathbf{z}^*}}{\eta_{\mathbf{z}^*}^T \Sigma \eta_{\mathbf{z}^*}} \cdot \min_{\eta_{\mathbf{z}^*} \neq 0} \frac{\eta_{\mathbf{z}^*}^T \Sigma \eta_{\mathbf{z}^*}}{\eta_{\mathbf{z}^*}^T \mathbf{M} \eta_{\mathbf{z}^*}} \\
&= \lambda_{\min}(\Sigma, \mathbf{M}) \cdot \min_{0 \neq \eta_{\mathbf{z}^*} \in T_{\mathbf{z}^*} \mathbb{S}_{\mathbf{xy}}} \frac{\eta_{\mathbf{z}^*}^T (\nabla^2 \bar{f}(\mathbf{z}^*) + \sigma_1 \cdot \Sigma) \eta_{\mathbf{z}^*}}{\eta_{\mathbf{z}^*}^T \Sigma \eta_{\mathbf{z}^*}} \\
&= \lambda_{\min}(\Sigma, \mathbf{M}) \cdot \min_{0 \neq \Sigma^{-\frac{1}{2}} \xi_{\mathbf{z}^*} \in T_{\mathbf{z}^*} \mathbb{S}_{\mathbf{xy}}} \frac{\xi_{\mathbf{z}^*}^T \Sigma^{-\frac{1}{2}} (\nabla^2 \bar{f}(\mathbf{z}^*) + \sigma_1 \cdot \Sigma) \Sigma^{-\frac{1}{2}} \xi_{\mathbf{z}^*}}{\xi_{\mathbf{z}^*}^T \xi_{\mathbf{z}^*}} \\
&= \lambda_{\min}(\Sigma, \mathbf{M}) \cdot \min_{0 \neq \Sigma^{-\frac{1}{2}} \xi_{\mathbf{z}^*} \in T_{\mathbf{z}^*} \mathbb{S}_{\mathbf{xy}}} \frac{\xi_{\mathbf{z}^*}^T \left(\Sigma^{-\frac{1}{2}} \nabla^2 \bar{f}(\mathbf{z}^*) \Sigma^{-\frac{1}{2}} + \sigma_1 \cdot \mathbf{I}_d \right) \xi_{\mathbf{z}^*}}{\xi_{\mathbf{z}^*}^T \xi_{\mathbf{z}^*}}
\end{aligned}$$

To bound the rightmost term, we first note that the eigenvalues of $\Sigma^{-\frac{1}{2}} \nabla^2 \bar{f}(\mathbf{z}^*) \Sigma^{-\frac{1}{2}}$ are $-\sigma_1 < -\sigma_2 \leq \dots \leq -\sigma_q \leq 0 \leq \dots \leq 0 \leq \sigma_q \leq \dots \leq \sigma_2 \leq \sigma_1$ (see (Golub and Zha, 1995)). So, the eigenvalue of $\Sigma^{-\frac{1}{2}} \nabla^2 \bar{f}(\mathbf{z}^*) \Sigma^{-\frac{1}{2}} + \sigma_1 \cdot \mathbf{I}_d$ are $0 < \sigma_1 - \sigma_2 \leq \dots \leq \sigma_1 - \sigma_q \leq \sigma_1 \leq \dots \leq \sigma_q + \sigma_1 \leq \dots \leq \sigma_2 + \sigma_1 \leq 2\sigma_1$. Furthermore, the null space of $\Sigma^{-\frac{1}{2}} \nabla^2 \bar{f}(\mathbf{z}^*) \Sigma^{-\frac{1}{2}} + \sigma_1 \cdot \mathbf{I}_d$ is exactly the space orthogonal to $\Sigma^{\frac{1}{2}} T_{\mathbf{z}^*} \mathbb{S}_{\mathbf{xy}}$, and this space is exactly the one dimensional subspace spanned by $\Sigma^{\frac{1}{2}} \mathbf{z}^*$. Indeed, since

$$\Sigma^{-\frac{1}{2}} \nabla^2 \bar{f}(\mathbf{z}^*) \Sigma^{-\frac{1}{2}} = \begin{bmatrix} & -\mathbf{R} \\ -\mathbf{R}^T & \end{bmatrix} \quad \text{and} \quad \Sigma^{\frac{1}{2}} \mathbf{z}^* = \begin{bmatrix} \tilde{\mathbf{u}}_1 \\ \tilde{\mathbf{v}}_1 \end{bmatrix}$$

(recall the definition of $\tilde{\mathbf{u}}_1$, $\tilde{\mathbf{v}}_1$, and \mathbf{R} in Eqs. (10) and (11)) we have

$$(\Sigma^{-\frac{1}{2}} \nabla^2 \bar{f}(\mathbf{z}^*) \Sigma^{-\frac{1}{2}} + \sigma_1 \cdot \mathbf{I}_d) \Sigma^{\frac{1}{2}} \mathbf{z}^* = \left(\begin{bmatrix} & -\mathbf{R} \\ -\mathbf{R}^T & \end{bmatrix} + \sigma_1 \mathbf{I} \right) \begin{bmatrix} \tilde{\mathbf{u}}_1 \\ \tilde{\mathbf{v}}_1 \end{bmatrix} = 0$$

where the last equality follows from the fact that $\begin{bmatrix} & \mathbf{R} \\ \mathbf{R}^T & \end{bmatrix}$ is the augmented matrix associated with \mathbf{R} , so $\begin{bmatrix} \tilde{\mathbf{u}}_1 \\ \tilde{\mathbf{v}}_1 \end{bmatrix}$, which has the dominant left and right singular vectors stacked, is the eigenvalue corresponding to the largest eigenvalue σ_1 . Noticing that $\Sigma^{-\frac{1}{2}} \nabla^2 \bar{f}(\mathbf{z}^*) \Sigma^{-\frac{1}{2}} + \sigma_1 \cdot \mathbf{I}_d$ is a symmetric matrix, and applying the Courant-Fisher theorem again, we find that

$$\min_{0 \neq \Sigma^{-\frac{1}{2}} \xi_{\mathbf{z}^*} \in T_{\mathbf{z}^*} \mathbb{S}_{\mathbf{xy}}} \frac{\xi_{\mathbf{z}^*}^T \left(\Sigma^{-\frac{1}{2}} \nabla^2 \bar{f}(\mathbf{z}^*) \Sigma^{-\frac{1}{2}} + \sigma_1 \cdot \mathbf{I}_d \right) \xi_{\mathbf{z}^*}}{\xi_{\mathbf{z}^*}^T \xi_{\mathbf{z}^*}} = \lambda_{d-1}(\Sigma^{-\frac{1}{2}} \nabla^2 \bar{f}(\mathbf{z}^*) \Sigma^{-\frac{1}{2}} + \sigma_1 \cdot \mathbf{I}_d) = \sigma_1 - \sigma_2$$

so

$$\lambda_{\min}(\text{Hess}f(\mathbf{z}^*)) \geq (\sigma_1 - \sigma_2) \cdot \lambda_{\min}(\Sigma, \mathbf{M}).$$

Using similar arguments, we find that

$$\lambda_{\max}(\text{Hess}f(\mathbf{z}^*)) \leq 2\sigma_1 \cdot \lambda_{\max}(\Sigma, \mathbf{M}).$$

We conclude by observing that

$$\kappa(\text{Hess}f(\mathbf{z}^*)) = \frac{\lambda_{\max}(\text{Hess}f(\mathbf{z}^*))}{\lambda_{\min}(\text{Hess}f(\mathbf{z}^*))} \leq \frac{2\sigma_1}{\sigma_1 - \sigma_2} \kappa(\Sigma, \mathbf{M})$$

E.4. Proof of Theorem 7

The costs are evident from the various formulas once we observe that none of the operations require forming \mathbf{S}_B or \mathbf{S}_w , but instead require taking product of these matrices with vectors. These products can be computed in cost proportional to the iterated products of the matrices $\hat{\mathbf{X}}$ and/or $\hat{\mathbf{Y}}$ with vectors. Computing a product of the matrix $\hat{\mathbf{X}}$ with a vector is equivalent to computing the product of the same vector with the matrices \mathbf{X} and \mathbf{Y} and subtracting the result. Computing the cost of the product of \mathbf{X} with a vector is proportional number of non-zeros in \mathbf{X} , and the cost of the product of \mathbf{Y} with a vector is $O(ld)$ since \mathbf{Y} has exactly l distinct rows (so we can compute only the product of the vector with each of these possible rows). Computing a product of the matrix $\hat{\mathbf{Y}}$ with a vector costs $O(ld)$ since the matrix is $l \times d$. Recall, that projections require normalization, but this again can be computed using iterated products with $\hat{\mathbf{X}}$.

The rest of the proof is devoted to proving the condition number bound, in a similar manner to the proof of Theorem 5. At the optimum \mathbf{w}^* , we have $-\mathbf{w}^{*\top} \mathbf{S}_B \mathbf{w}^* = -\rho_1$, and the Riemannian gradient vanishes (since it is a critical point), i.e. $\text{grad} f(\mathbf{w}^*) = 0$. So, the Riemannian Hessian at \mathbf{w}^* reduces to

$$\text{Hess} f(\mathbf{w}^*) [\eta_{\mathbf{w}^*}] = \mathbf{P}_{\mathbf{w}^*} \mathbf{M}^{-1} (-\mathbf{S}_B + \rho_1 \cdot (\mathbf{S}_w + \lambda \mathbf{I}_d)) \eta_{\mathbf{w}^*}.$$

The Riemannian Hessian is self-adjoint with respect to the Riemannian metric (see Absil et al. (2009), Proposition 5.5.3), so for every $\mathbf{w} \in \mathbb{S}^{\mathbf{S}_w + \lambda \mathbf{I}_d}$ we have $g_{\mathbf{x}}(\text{Hess} f(\mathbf{w})[\eta], \xi) = g_{\mathbf{x}}(\eta, \text{Hess} f(\mathbf{w})[\xi])$ for any $\eta, \xi \in T_{\mathbf{w}} \mathbb{S}^{\mathbf{S}_w + \lambda \mathbf{I}_d}$. So, due to the Courant-Fisher Theorem we have

$$\begin{aligned} \lambda_{\max}(\text{Hess} f(\mathbf{w}^*)) &= \max_{0 \neq \eta_{\mathbf{w}^*} \in T_{\mathbf{w}^*} \mathbb{S}^{\mathbf{S}_w + \lambda \mathbf{I}_d}} \frac{g_{\mathbf{w}^*}(\eta_{\mathbf{w}^*}, \text{Hess} f(\mathbf{w}^*)[\eta_{\mathbf{w}^*}])}{g_{\mathbf{w}^*}(\eta_{\mathbf{w}^*}, \eta_{\mathbf{w}^*})} \\ \lambda_{\min}(\text{Hess} f(\mathbf{w}^*)) &= \min_{0 \neq \eta_{\mathbf{w}^*} \in T_{\mathbf{w}^*} \mathbb{S}^{\mathbf{S}_w + \lambda \mathbf{I}_d}} \frac{g_{\mathbf{w}^*}(\eta_{\mathbf{w}^*}, \text{Hess} f(\mathbf{w}^*)[\eta_{\mathbf{w}^*}])}{g_{\mathbf{w}^*}(\eta_{\mathbf{w}^*}, \eta_{\mathbf{w}^*})} \end{aligned}$$

The above is stated in a coordinate-free manner. In ambient coordinates, viewing $T_{\mathbf{z}^*} \mathbb{S}^{\mathbf{S}_w + \lambda \mathbf{I}_d}$ as a subspace of \mathbb{R}^d (see Eq. (3)):

$$\begin{aligned} \lambda_{\max}(\text{Hess} f(\mathbf{w}^*)) &= \max_{0 \neq \eta_{\mathbf{w}^*} \in T_{\mathbf{w}^*} \mathbb{S}^{\mathbf{S}_w + \lambda \mathbf{I}_d}} \frac{(\eta_{\mathbf{w}^*}, \text{Hess} f(\mathbf{w}^*)[\eta_{\mathbf{w}^*}])_{\mathbf{M}}}{(\eta_{\mathbf{w}^*}, \eta_{\mathbf{w}^*})_{\mathbf{M}}} \\ \lambda_{\min}(\text{Hess} f(\mathbf{z}^*)) &= \min_{0 \neq \eta_{\mathbf{w}^*} \in T_{\mathbf{w}^*} \mathbb{S}^{\mathbf{S}_w + \lambda \mathbf{I}_d}} \frac{(\eta_{\mathbf{w}^*}, \text{Hess} f(\mathbf{w}^*)[\eta_{\mathbf{w}^*}])_{\mathbf{M}}}{(\eta_{\mathbf{w}^*}, \eta_{\mathbf{w}^*})_{\mathbf{M}}} \end{aligned}$$

Plugging in the ambient coordinates formula for the Hessian, the quotient in the above reduces to

$$\frac{\eta_{\mathbf{w}^*}^{\top} \mathbf{M} \mathbf{P}_{\mathbf{w}^*} \mathbf{M}^{-1} (-\mathbf{S}_B + \rho_1 \cdot (\mathbf{S}_w + \lambda \mathbf{I}_d)) \eta_{\mathbf{w}^*}}{\eta_{\mathbf{w}^*}^{\top} \mathbf{M} \eta_{\mathbf{w}^*}}.$$

Now using $\mathbf{M} \mathbf{P}_{\mathbf{w}^*} \mathbf{M}^{-1} = \mathbf{P}_{\mathbf{w}^*}^{\top}$ and the fact that $\mathbf{P}_{\mathbf{w}^*}$ is a projection on $T_{\mathbf{w}^*} \mathbb{S}^{\mathbf{S}_w + \lambda \mathbf{I}_d}$ so $\mathbf{P}_{\mathbf{w}^*} \eta_{\mathbf{w}^*} = \eta_{\mathbf{w}^*}$ (since $\eta_{\mathbf{w}^*} \in T_{\mathbf{w}^*} \mathbb{S}^{\mathbf{S}_w + \lambda \mathbf{I}_d}$), we further see that

$$\begin{aligned} \frac{\eta_{\mathbf{w}^*}^{\top} \mathbf{M} \mathbf{P}_{\mathbf{w}^*} \mathbf{M}^{-1} (-\mathbf{S}_B + \rho_1 \cdot (\mathbf{S}_w + \lambda \mathbf{I}_d)) \eta_{\mathbf{w}^*}}{\eta_{\mathbf{w}^*}^{\top} \mathbf{M} \eta_{\mathbf{w}^*}} &= \\ \frac{\eta_{\mathbf{w}^*}^{\top} (-\mathbf{S}_B + \rho_1 \cdot (\mathbf{S}_w + \lambda \mathbf{I}_d)) \eta_{\mathbf{w}^*}}{\eta_{\mathbf{w}^*}^{\top} \mathbf{M} \eta_{\mathbf{w}^*}} &= \\ \frac{\eta_{\mathbf{w}^*}^{\top} (-\mathbf{S}_B + \rho_1 \cdot (\mathbf{S}_w + \lambda \mathbf{I}_d)) \eta_{\mathbf{w}^*}}{\eta_{\mathbf{w}^*}^{\top} (\mathbf{S}_w + \lambda \mathbf{I}_d) \eta_{\mathbf{w}^*}} \cdot \frac{\eta_{\mathbf{w}^*}^{\top} (\mathbf{S}_w + \lambda \mathbf{I}_d) \eta_{\mathbf{w}^*}}{\eta_{\mathbf{w}^*}^{\top} \mathbf{M} \eta_{\mathbf{w}^*}}. \end{aligned}$$

(where we use the fact that $\mathbf{S}_w + \lambda \mathbf{I}_d$ is not singular).

Denote $\tilde{\lambda}_{\min} = \lambda_{\min}(\mathbf{S}_w + \lambda \mathbf{I}_d, \mathbf{M})$ and $\tilde{T}_{w^*} \mathbb{S}^{\mathbf{S}_w + \lambda \mathbf{I}_d} = (\mathbf{S}_w + \lambda \mathbf{I}_d)^{\frac{1}{2}} T_{w^*} \mathbb{S}^{\mathbf{S}_w + \lambda \mathbf{I}_d}$. We have,

$$\begin{aligned}
\lambda_{\min}(\text{Hess}f(\mathbf{w}^*)) &\geq \min_{0 \neq \eta_{w^*} \in T_{w^*} \mathbb{S}^{\mathbf{S}_w + \lambda \mathbf{I}_d}} \frac{\eta_{w^*}^T (-\mathbf{S}_B + \rho_1 \cdot (\mathbf{S}_w + \lambda \mathbf{I}_d)) \eta_{w^*}}{\eta_{w^*}^T (\mathbf{S}_w + \lambda \mathbf{I}_d) \eta_{w^*}} \cdot \min_{\eta_{w^*} \neq 0} \frac{\eta_{w^*}^T (\mathbf{S}_w + \lambda \mathbf{I}_d) \eta_{w^*}}{\eta_{w^*}^T \mathbf{M} \eta_{w^*}} \\
&= \tilde{\lambda}_{\min} \cdot \min_{0 \neq \eta_{w^*} \in T_{w^*} \mathbb{S}^{\mathbf{S}_w + \lambda \mathbf{I}_d}} \frac{\eta_{w^*}^T (-\mathbf{S}_B + \rho_1 \cdot (\mathbf{S}_w + \lambda \mathbf{I}_d)) \eta_{w^*}}{\eta_{w^*}^T (\mathbf{S}_w + \lambda \mathbf{I}_d) \eta_{w^*}} \\
&= \tilde{\lambda}_{\min} \cdot \min_{0 \neq \xi_{w^*} \in \tilde{T}_{w^*} \mathbb{S}^{\mathbf{S}_w + \lambda \mathbf{I}_d}} \frac{\xi_{w^*}^T (\mathbf{S}_w + \lambda \mathbf{I}_d)^{-\frac{1}{2}} (-\mathbf{S}_B + \rho_1 \cdot (\mathbf{S}_w + \lambda \mathbf{I}_d)) (\mathbf{S}_w + \lambda \mathbf{I}_d)^{-\frac{1}{2}} \xi_{w^*}}{\xi_{w^*}^T \xi_{w^*}} \\
&= \tilde{\lambda}_{\min} \cdot \min_{0 \neq \xi_{w^*} \in \tilde{T}_{w^*} \mathbb{S}^{\mathbf{S}_w + \lambda \mathbf{I}_d}} \frac{\xi_{w^*}^T \left(-(\mathbf{S}_w + \lambda \mathbf{I}_d)^{-\frac{1}{2}} \mathbf{S}_B (\mathbf{S}_w + \lambda \mathbf{I}_d)^{-\frac{1}{2}} + \rho_1 \cdot \mathbf{I}_d \right) \xi_{w^*}}{\xi_{w^*}^T \xi_{w^*}}
\end{aligned}$$

To bound the rightmost term, we first note that the eigenvalues of $(\mathbf{S}_w + \lambda \mathbf{I}_d)^{-\frac{1}{2}} \mathbf{S}_B (\mathbf{S}_w + \lambda \mathbf{I}_d)^{-\frac{1}{2}}$ are the generalized eigenvalues of the matrix pencil $(\mathbf{S}_B, \mathbf{S}_w + \lambda \mathbf{I})$, i.e., $\rho_1 > \rho_2 \geq \dots \geq \rho_d = 0$. So, the eigenvalue of $-(\mathbf{S}_w + \lambda \mathbf{I}_d)^{-\frac{1}{2}} \mathbf{S}_B (\mathbf{S}_w + \lambda \mathbf{I}_d)^{-\frac{1}{2}} + \rho_1 \cdot \mathbf{I}_d$ are $0 < \rho_1 - \rho_2 \leq \dots < \rho_1$. Furthermore, the null space of $-(\mathbf{S}_w + \lambda \mathbf{I}_d)^{-\frac{1}{2}} \mathbf{S}_B (\mathbf{S}_w + \lambda \mathbf{I}_d)^{-\frac{1}{2}} + \rho_1 \cdot \mathbf{I}_d$ is exactly the space orthogonal to $\tilde{T}_{w^*} \mathbb{S}^{\mathbf{S}_w + \lambda \mathbf{I}_d}$, and this space is exactly the one dimensional subspace spanned by $(\mathbf{S}_w + \lambda \mathbf{I}_d)^{\frac{1}{2}} \mathbf{w}^*$. Indeed, since \mathbf{w}^* is the generalized eigenvector of the matrix pencil $(\mathbf{S}_B, \mathbf{S}_w + \lambda \mathbf{I})$ corresponding to the generalized eigenvalue ρ_1 , then since $\mathbf{S}_w + \lambda \mathbf{I}_d$ is not singular, \mathbf{w}^* is also the eigenvector of the matrix $(\mathbf{S}_w + \lambda \mathbf{I}_d)^{-1} \mathbf{S}_B$ corresponding to the eigenvalue ρ_1 :

$$\begin{aligned}
&(-(\mathbf{S}_w + \lambda \mathbf{I}_d)^{-\frac{1}{2}} \mathbf{S}_B (\mathbf{S}_w + \lambda \mathbf{I}_d)^{-\frac{1}{2}} + \rho_1 \cdot \mathbf{I}_d) (\mathbf{S}_w + \lambda \mathbf{I}_d)^{\frac{1}{2}} \mathbf{w}^* = \\
&-(\mathbf{S}_w + \lambda \mathbf{I}_d)^{\frac{1}{2}} (\mathbf{S}_w + \lambda \mathbf{I}_d)^{-1} \mathbf{S}_B \mathbf{w}^* + \rho_1 \cdot (\mathbf{S}_w + \lambda \mathbf{I}_d)^{\frac{1}{2}} \mathbf{w}^* = 0.
\end{aligned}$$

Noticing that $-(\mathbf{S}_w + \lambda \mathbf{I}_d)^{-\frac{1}{2}} \mathbf{S}_B (\mathbf{S}_w + \lambda \mathbf{I}_d)^{-\frac{1}{2}} + \rho_1 \cdot \mathbf{I}_d$ is a symmetric matrix, and applying the Courant-Fisher theorem again, we find that

$$\begin{aligned}
&\min_{0 \neq \xi_{w^*} \in \tilde{T}_{w^*} \mathbb{S}^{\mathbf{S}_w + \lambda \mathbf{I}_d}} \frac{\xi_{w^*}^T \left(-(\mathbf{S}_w + \lambda \mathbf{I}_d)^{-\frac{1}{2}} \mathbf{S}_B (\mathbf{S}_w + \lambda \mathbf{I}_d)^{-\frac{1}{2}} + \rho_1 \cdot \mathbf{I}_d \right) \xi_{w^*}}{\xi_{w^*}^T \xi_{w^*}} = \\
&\lambda_{d-1}(-(\mathbf{S}_w + \lambda \mathbf{I}_d)^{-\frac{1}{2}} \mathbf{S}_B (\mathbf{S}_w + \lambda \mathbf{I}_d)^{-\frac{1}{2}} + \rho_1 \cdot \mathbf{I}_d) = \rho_1 - \rho_2
\end{aligned}$$

so

$$\lambda_{\min}(\text{Hess}f(\mathbf{w}^*)) \geq (\rho_1 - \rho_2) \cdot \lambda_{\min}(\mathbf{S}_w + \lambda \mathbf{I}_d, \mathbf{M}).$$

Using similar arguments, we find that

$$\lambda_{\max}(\text{Hess}f(\mathbf{w}^*)) \leq \rho_1 \cdot \lambda_{\max}(\mathbf{S}_w + \lambda \mathbf{I}_d, \mathbf{M}).$$

We conclude by observing that

$$\kappa(\text{Hess}f(\mathbf{w}^*)) = \frac{\lambda_{\max}(\text{Hess}f(\mathbf{w}^*))}{\lambda_{\min}(\text{Hess}f(\mathbf{w}^*))} \leq \frac{\rho_1}{\rho_1 - \rho_2} \cdot \kappa(\mathbf{S}_w + \lambda \mathbf{I}_d, \mathbf{M}),$$

E.5. Proof of Lemma 8

The argument is rather standard and appeared in similar forms in the literature. For $\kappa(\mathbf{Z}^T \mathbf{Z} + \lambda \mathbf{I}, \mathbf{Z}^T \mathbf{S}^T \mathbf{S} \mathbf{Z} + \lambda \mathbf{I}) \leq 3$ to hold, it is enough to show that

$$\frac{1}{2}(\mathbf{Z}^T \mathbf{Z} + \lambda \mathbf{I}) \preceq \mathbf{Z}^T \mathbf{S}^T \mathbf{S} \mathbf{Z} + \lambda \mathbf{I} \preceq \frac{3}{2}(\mathbf{Z}^T \mathbf{Z} + \lambda \mathbf{I}).$$

Let $\mathbf{Z} = \mathbf{Q} \mathbf{R}$ be a λ -QR factorization of \mathbf{Z} (see [Avron et al. \(2017\)](#) for a definition). Multiplying by \mathbf{R}^{-1} on both sides, we find it suffices to show that with probability of at least $1 - \delta$ we have

$$\frac{1}{2} \mathbf{I}_d \preceq \mathbf{Q}^T \mathbf{S}^T \mathbf{S} \mathbf{Q} + \lambda \mathbf{R}^{-T} \mathbf{R}^{-1} \preceq \frac{3}{2} \mathbf{I}_d$$

or, equivalently,

$$\|\mathbf{Q}^T \mathbf{S}^T \mathbf{S} \mathbf{Q} + \lambda \mathbf{R}^{-T} \mathbf{R}^{-1} - \mathbf{I}_d\|_2 \leq \frac{1}{2}.$$

Since $\mathbf{Q}^T \mathbf{S}^T \mathbf{S} \mathbf{Q} + \lambda \mathbf{R}^{-T} \mathbf{R}^{-1} - \mathbf{I}_d = \mathbf{Q}^T \mathbf{S}^T \mathbf{S} \mathbf{Q} - \mathbf{Q}^T \mathbf{Q}$ ([Avron et al., 2017](#)) and the spectral norm dominates the Frobenius norm, it is enough to show that

$$\|\mathbf{Q}^T \mathbf{S}^T \mathbf{S} \mathbf{Q} - \mathbf{Q}^T \mathbf{Q}\|_F \leq \frac{1}{2}.$$

It is known ([Avron et al., 2014b](#)) that for any two fixed matrices \mathbf{A} and \mathbf{B} , and a COUNTSKETCH matrix \mathbf{S}_0 with $m \geq 5/(\epsilon^2 \delta)$ rows, we have that with probability of at least $1 - \delta$,

$$\|\mathbf{A}^T \mathbf{S}_0^T \mathbf{S}_0 \mathbf{B} - \mathbf{A}^T \mathbf{B}\|_F \leq \epsilon \cdot \|\mathbf{A}\|_F \cdot \|\mathbf{B}\|_F.$$

Since $\|\mathbf{Q}\|_F^2 = s_\lambda(\mathbf{Z})$ ([Avron et al., 2017](#)), then with $s \geq 20s_\lambda(\mathbf{Z})^2/\delta$ we have

$$\|\mathbf{Q}^T \mathbf{S}^T \mathbf{S} \mathbf{Q} - \mathbf{Q}^T \mathbf{Q}\|_F \leq \frac{1}{2}$$

with probability of at least $1 - \delta$.